2015

The gliding mechanism of diatoms

Department of Picobiology, Graduate School of Life Science, University of Hyogo

Nozomi Yamaoka

Table of Contents

Abstract

Some unicellular pennate diatoms can move over the substratum and this motion called gliding has been known for long time. However, the molecular mechanism of this motion was not understood well. It is also true for unique gliding motion of a colonial pennate diatom, *Bacillaria paxillifer*, in which a pair of two adjacent cells in a colony glide with each other. Here, I report morphological and biochemical analyses of two kinds of diatoms, unicellular *Pleurosigma* sp. and colonial *B. paxillifer*. First, I carried out quantitative analyses of gliding motion of *B. paxillifer* and morphological analyses of this diatom. I demonstrated involvement of the actomyosin system in gliding motion of this diatom using actomyosin inhibitors, and observed actin bundles by fluorescence-labeled phalloidin staining. I also found the actin-like filaments near the raphe, where the adjacent cells attach to each other, and novel electron-dense structures located between the plasma membrane and these actin-like filaments. These results indicated that gliding motion of *B. paxillifer* is powered by the actomyosin system as proposed in unicellular gliding diatoms. Second, I performed biochemical search to identify a putative motor protein(s) to drive gliding motion in a unicellular diatom, *Pleurosigma* sp. because there was no biochemical information of such a motor protein(s) despite the fact that the pivotal role of actin filaments in gliding of unicellular diatoms has been postulated. I found a 130 kDa actin-binding polypeptide that has some myosin-like features. Immunofluorescence microscopy with a monoclonal antibody against this 130 kDa polypeptide demonstrated its localization along the raphe even in the absence of the actin bundles, suggesting that the protein forms linkage between the actin filaments and the plasma membrane. From these results, I proposed that the 130 kDa polypeptide is a candidate for a motor protein

that powers gliding motion in the unicellular diatom. Third, I investigated saccharide components of extracellular mucilage both in *Pleurosigma* sp. and in *B. paxillifer*. It has been postulated that gliding motion of diatoms depends on extracellular mucilage and its movement is driven by intracellular actomyosin, but there is no direct observation of mucilage movement during gliding in living diatoms. Here, I described some characteristics of movement of mucilage secreted from *Pleurosigma* sp. and *B. paxillifer* using fluorescein-labeled lectins. I also found that mucilage of these two kinds of diatoms has different saccharide compositions. Finally, I will discuss, from these findings and previous observations, common and different points of gliding mechanism and its regulation between the unicellular and colonial diatoms.

Publication list

Yamaoka Nozomi, Suetomo Yasutaka, Yoshihisa Tohru and Sonobe Seiji. (2016). Motion analysis and ultrastructural study of a colonial diatom, *Bacillaria paxillifer*. *Microscopy* (Oxf). (inpress)

Acknowledgments

I am especially grateful to Prof. Tohru Yoshihisa for helpful discussion and supporting this thesis and comments on my experiments, to Dr. Seiji Sonobe for teaching pleasure of experiments and helpful comments, to Dr. Etsuo Yokota for discussion and teaching research skills and to Dr. Teruo Shimmen for helpful comments. I am very grateful to Prof. Tobias Baskin (University of Massachusetts) for helpful comments, advice and receiving my request for studying abroad, to Dr. Toshinobu Suzaki (Kobe University) for having invited me to the world protistology, to Dr. Yasutaka Suetomo (Iwakuni City Microlife Museum) for helpful advice regarding getting and culturing diatoms, to Dr. Kei Kimura (Saga University) for instructing the method on TEM sample preparation, to Dr. Yuri Nishino and Prof. Atsuo Miyazawa for SEM sample preparation and for allowing operation of the equipment and to Dr. Shigenobu Yonemura (RIKEN CDB) for allowing operation of laser experiment, to Dr. Kazuhiro Oiwa (National Institute of Information and Communications Technology) for helpful comments and advice, to Dr. Hiroaki Kojima for teaching experiment and helpful comments, to Dr. Tadashi Matsukawa for teaching experiments using glass needle. My thanks are also to Prof. Makoto Miyata (Osaka City University), to Dr. Eisaku Katayama and to Dr. Yu-hei Tahara for teaching the freeze fracture electron microscopy. I thank Dr. Yasuhiro Kamei (National Institute for Basic Biology) for generous gift micro beads, Dr. Yumiko Makino (National Institute for Basic Biology) for analyses of amino acid sequences, Dr. Yukinori Nishigami (Kyoto University) for helpful comments and advice and Dr. Atsushi Taniguti (National Institute for Basic Biology) for technical help. I also thank Kengo Arima, Ryuji Yanase and Go Kobashigawa and other members of our laboratory.

List of Abbreviations

ASW: artificial seawater

ATP: adenosine triphosphate

BDM: 2, 3-butanedione monoxime

BSA: bovine serum albumin

CBB: coomassie brilliant blue

CCD: charge coupled device

Con A: concanavalin A

DMSO: dimethyl sulfoxide

DTT: threo-1,4,-dimercapto-2,3-butanediol

EGTA: *O*,*O*'-*bis*(2-aminoethyl)ethylene glycol-*N*,*N*,*N*',*N*'-tetraacetic acid

PBS: phosphate-buffered saline

PI: protease inhibitor

PIPES: piperazine-1,4-*bis*(2-ethanesulfonic acid)

PMSF: phenylmethylsulfonyl fluoride

PVDF: polyvinylidene difluoride

SDS-PAGE: sodium dodecyl sulfate-polyacrylamide gel electronphoresis

SEM: scanning electron microscopy

S-WGA: succinylated wheat germ agglutinin

TEM: transmission electron microscopy

Chapter 1

General Introduction

1-1 General introduction

Diatoms are one of the most abundant clades of phytoplankton. They bear the important role in the food chain, producing primary products as producers. Diatoms inhabit the ocean, brackish waters, freshwater and sometimes in semi-aquatic environments like wetlands. There are many kinds of species in living and also fossil diatoms. Diatoms are classified into two major orders by their cell shapes, that is, centric diatoms that have radially symmetrical shapes and pennate diatoms that have bilaterally symmetrical shape. Both orders of diatoms are basically unicellular, but some species can exist as colonies in the shape of filaments, fans, sheets, or stars.

The most striking feature of diatoms is that the cell is encased in a highly silicified cell wall, named a frustule. In general, the frustule comprises two nesting halves, termed epi- and hypo-valves, and girdle bands. Each species has its own shape of the silicified cell wall. In some pennate diatoms, the valve has a long slit, called a raphe, which is often divided into two parts by a central nodule. These diatoms can adhere to the substratum and move bi-directionally over the substratum. Although this motility, called gliding, has been known for a long time, the first observation of this motion was recorded by O. F. Müller, a Danish naturalist, in 1780s (Mùller, 1782; 1783). He described the movement of a colonial diatom, *Bacillaria paxillifer*. After his observation, many researchers reported the gliding motion of diatoms and measured the gliding force in 1960s and tried to solve the gliding mechanism in 1980s. Its mechanism and physiological significance have not been completely understood (Edgar and Pickett-Heaps, 1984; Wetherbee *et al*., 1998). Gliding is propelled without cilia, flagella, or cell deformation as observed in amoeboids. The velocity is relatively high, ranging from 1 to 25 μm/s depending upon species and conditions (Edgar, 1979; Round *et al*., 1990; Gupta and

Agrawal, 2007).

In the unicellular gliding diatoms, electron and fluorescence microscopy revealed that a pair of actin bundles is present under the plasma membrane facing toward the raphe (Edgar and Pickett-Heaps, 1983; Edgar and Zavortink, 1983; Poulsen *et al*., 1999). Because gliding of unicellular pennate diatoms is inhibited by actin inhibitors, such as cytochalasin A and latrunculin A, and by a myosin inhibitor, 2,3-butanedione monoxime (BDM), gliding is thought to be driven by the actomyosin system (Poulsen *et al*., 1999). The unicellular gliding diatoms leave a trail of adhesive mucilage behind them on the substratum when gliding (Drum and Hopkins, 1966; Pickett-Heaps *et al*., 1991; Lind *et al*., 1997). Mucilage is thought to be secreted near the raphe by exocytosis and to link the cell body to the substratum accompanied by movement along the raphe (Edgar and Pickett-Heaps, 1982; 1983; Edgar, 1983; Webster *et al*., 1985; McConville *et al*., 1999). When mucilage arrives at the end of the raphe, the mucilage seems to be cut by the polar fissure, a specific structure of the frustule, and remains on the substratum leaving a trace of the gliding motion (Edgar and Pickett-Heaps, 1983). Thus, involvement of mucilage in gliding is also postulated.

The following hypothesis for gliding motion has been proposed (Fig. 1; Edgar and Pickett-Heaps, 1983; Wetherbee *et al*., 1998). The gliding of these unicellular diatoms is hypothesized to be driven by a myosin motor running along the two actin bundles aligned on the raphe. The motility force is then transmitted to the cell exterior by a putative transmembrane protein(s) that links the motor complex and mucilage bound to the substratum. Involvement of this putative myosin is supported by an experiment with BDM, and various putative myosins were annotated in the whole-genome projects of *Phaeodactylum tricornutum* and *Thalassiosira pseudonana* (Heintzelman and Enriquez,

2010), but it remains to be addressed which myosin homolog is responsible for gliding motion. Moreover, biochemical studies on diatom myosins have not been carried out.

Furthermore, there remain many unexplained mysteries in gliding motion of diatoms. How is bi-directionality of the gliding achieved; diatoms use two actin tracts with opposite polarities and one motor, or use actin tracts with single polarity and two kinds of motors moving in opposite directions? How is mucilage involved in gliding? Mucilage is thought to be secreted from the raphe and moved by actomyosin, but there is no direct evidence for this notion, and behavior of mucilage has not been observed in living diatoms.

In addition to the unicellular diatoms, the colonial gliding diatom, *Bacillaria paxillifer*, was known by its gliding between adjacent cells, but the molecular mechanism of this unique gliding is not understood. Schmid (2007) reported that mucilage of *B. paxillifer* extends from the raphe and links the two adjacent cells, which is equivalent to relation between a cell and the opposing substratum in unicellular diatoms. I believe that comparing gliding motion between unicellular and colonial diatoms should contribute to elucidation of gliding mechanism and physiological meanings of gliding.

In this thesis, I report (1) structural analyses on actin-like filaments and a novel structure in colonial diatom, *Bacillaria paxillifer*; (2) biochemical analyses on an actin-binding protein in a unicellular diatom, *Pleurosigma* sp. and; (3) real time observation of movement of secreted mucilage in both diatoms during gliding using fluorescent lectins.

1-2 Figure

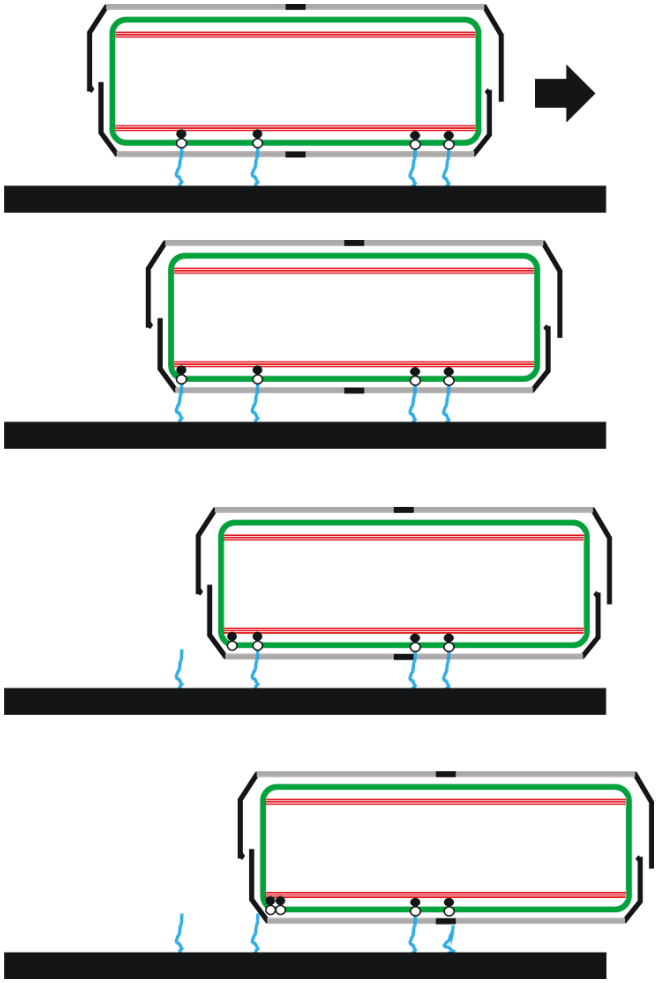

Fig. 1. A schematic view of the hypothesis of gliding motion of unicellular diatoms. Actin bundles (red) locate along the both raphes (gray part of blacked cell wall) and mucilage (blue) is secreted to exterior through the raphe. Secreted mucilage is moved by a putative motor protein(s) (filled circles associated with actin) through a putative transmembrane protein(s) (open circles next to the motor protein). Because mucilage was fixed to the substratum (wide black line), the cell moves on the substratum. At the end of a cell, mucilage is cut and deposited as a trail. Figure redrawn from the suggesting motility model (Wetherbee *et al*., 1998).

Chapter 2

Gliding mechanism of the colonial diatom,

Bacillaria paxillifer

2-1 Introduction

The pennate diatom, *Bacillaria paxillifer*, forms a colony consisting of two to dozens of cells, and adjacent cells slide with each other (*i.e.*, each cell glides on the surface of the neighboring cell but not on the substratum), resulting in stretching and shrinking of the colony. In spite of the fact that *B. paxillifer* is the first diatom in which gliding has been described (Mùller, 1782; 1783), its mechanism and physiological significance have not been understood well (Kapinga and Gordon, 1992).

Valves of *B. paxillifer* have two characteristic structures, that is, one continuous linear raphe on each valve, which is not divided by the central nodule, and fibulae, arch-shaped structures crossing over the raphe in the interior side of the valves (Jahn and Schmid, 2007; Schmid, 2007). Schmid (2007) reported that each cells in a colony are connected to adjacent cells by an electron-lucent material, which is thought to be mucilage, but not by rigid structures on the valve. However, the positional relationship of these structures and cytoskeletal elements has not been demonstrated. On one hand, there is no report on the mechanism of motive force generation in gliding motion of *B. paxillifer* so far. On the other hand, the involvement of actomyosin in intra-colonial gliding is reasonable, because of its important role in gliding of unicellular diatoms (Edgar and Pickett-Heaps, 1983; 1984; Poulsen *et al*., 1999). In this chapter, I describe quantitative analysis of the gliding motion in *B. paxillifer* under several physiological conditions and morphological studies using light and electron microscopy.

2-2 Materials and Methods

Cell culture

B. paxillifer (O. F. Mùller) was isolated from the sea coast in Iwakuni City, Japan. Cells were cultured in Daigo's Artificial Seawater SP (Nihon Pharmaceutical, Tokyo, Japan) containing Daigo's IMK Medium (IMK Medium; Nihon Pharmaceutical) and Na_2SiO_3 (Wako, Osaka, Japan) as a source of silicate. The culture was maintained at 25°C under an 18-h light/6-h dark cycle with light supplied by fluorescent lamps at 9.4 μmol/(m^2s).

Motion recording and quantification

Movement of *B. paxillifer* cells cultured in ASW at room temperature on an uncoated glass slide under continuous illumination was recorded under a bright-field microscope, BX-50 (Olympus, Tokyo, Japan) with a CCD camera, Victor KY-F550 (JVC Kenwood, Kanagawa, Japan), and DV Link (JVC Kenwood) as a recording software. Frames with a defined interval were extracted from a digital movie recording of the cell motion, and the distance between tips of a pair of adjacent cells in a colony was measured. When the recording showed that the tips of the two cells were closest, the distance was set to 0 μm. Relative velocity was calculated from the difference of distances between two neighbors of the extracted frames divided by the time interval of these two frames. All of the quantitative analyses of cell motion were performed with the NIH ImageJ software (Rasband, 1997-2014).

Actin and myosin inhibitors

Latrunculin B (Wako) was dissolved in dimethyl sulfoxide (DMSO; Wako) to

make a 1 mM stock solution and was stored at −20°C. The stock solution was diluted in ASW to 5 μM, and cells on a glass slide were soaked in this working solution by perfusion. After confirming the inhibition of gliding motion (within 1 min), the cells were rinsed with ASW several times by perfusion to remove latrunculin B, if necessary. BDM (Sigma-Aldrich, St. Louis, MO, USA) was dissolved in DMSO to make a 5 M stock solution and was stored at −20°C. The stock solution was added to the culture medium to give a final concentration of 50 mM. If necessary, BDM was removed by washing the cells with ASW several times. In all experiments, controls received equivalent volumes of DMSO. These cells were observed under the bright-field microscope as described above.

Fluorescence microscopy

For phalloidin staining, cells were fixed with 3.6% w/v formaldehyde (Wako) in phosphate-buffered saline (PBS) for 60 min, permeabilized with 0.02% w/v Triton X-100 in PBS, and stained with 33 nM Alexa Fluor 488-labeled phalloidin (Invitrogen, Carlsbad, CA, USA) at room temperature. Samples were observed with an epifluorescence microscope, BX-50 (Olympus), equipped with a CCD camera, DP70 (Olympus).

Electron microscopy

For the scanning electron microscopy (SEM) analysis, cells were fixed with 2.5% w/v glutaraldehyde (Nisshin EM, Tokyo, Japan) and 2% w/v paraformaldehyde (Wako) in 40 mM sodium cacodylate (Wako) buffer at pH 7.0 on ice for 120 min. After the prefixed cells were rinsed in 40 mM sodium cacodylate buffer, the cells were postfixed with 2% w/v OsO_4 (Nisshin EM) in 40 mM sodium cacodylate buffer at pH 7.0 on ice for

120 min. The cells attached to a round coverslip with a diameter of 5 mm coated with 0.5% w/v polyethyleneimine were dehydrated with ethanol, subsequently infiltrated with *t*-butyl alcohol (Wako) at room temperature, and finally freeze-dried as described previously (Inoue and Osatake, 1988). Specimens were coated with carbon and platinum in series by evaporation (C) and sputtering (Pt). Images of the specimens were obtained with a field emission-scanning electron microscope, JSM-6701F (JEOL, Akishima, Japan).

For observation of intracellular structures by SEM, cells were fixed with 3.6% w/v formaldehyde for 60 min at room temperature and sonicated (Tomy Ultrasonic Disruptor UD-201; Tomy Seiko, Tokyo, Japan) using "output 2" and "duty 30" settings. Fractured cells were washed with PBS several times to remove the cytoplasm, dehydrated, dried, coated, and observed as described above.

For the transmission electron microscopy (TEM) analysis, cells were treated as follows for fixation: 1.25% w/v glutaraldehyde and 1% w/v paraformaldehyde in ASW on ice for 30 min; 2.5% w/v glutaraldehyde, 2% w/v paraformaldehyde, and 0.5% w/v tannic acid (Merck, Kenilworth, NJ, USA) in 40 mM sodium cacodylate buffer at pH 7.0 on ice for 90 min; and 2% w/v OsO_4 in the same buffer on ice for 120 min. The fixed cells were dehydrated in acetone on ice and embedded in Spurr's resin (Stansted, Essex, United Kingdom) at room temperature, and the resulting resin block was ultrathin-sectioned with an ultramicrotome (Reichert-Nissei Ultracuts; Leica Microsystems, Wetzlar, Germany). Details of TEM fixation were described previously (Kimura and Tomaru, 2015). Ultrathin sections were collected on a one-hole copper mesh grid, stained with 6% w/v uranyl acetate (EMS, Hatfield, PA, USA) for 15 min and then with lead citrate solution as described previously (Reynolds, 1963) for 10 min, and observed with

a transmission electron microscope, JEM-1200 EXII (JEOL) at 80 kV.

2-3 Results

2-3-1 Motion analysis of *B. paxillifer*

I first recorded and quantitated the gliding of *B. paxillifer* under the bright-field microscope. Two adjacent cells in a *B. paxillifer* colony underwent active gliding together under preferable growth conditions (Fig. 2-1a). When a colony was fully extended, the cells were arranged in a straight line and then began to shrink in the opposite direction. Cells sometimes turned back prior to full extension. When colonies shrank, some of them rotated and changed their axis of gliding. These extending and shrinking patterns usually were repeated. As the number of cells in a colony increased, the shape of the colony tended to become zigzag. That also appeared to be true when colonies contained dividing cells.

Fig. 2-1b shows a quantitative analysis of gliding. I measured the distance between the tips of one pair of adjacent cells in a *B. paxillifer* colony and plotted them against time. The reciprocal movement of this pair of cells was cyclic, with a period of 35.0 ± 1.5 s. Gliding periods of adjacent cells in the same colony were fairly constant; the periods fell within a range of a few seconds of each other. On the other hand, the values varied from a few sec to tens of seconds among different colonies. Usually, gliding velocity became maximal when the tip distance between the two adjacent cells approached 0, and gliding decelerated as the two tips pulled apart. The maximal velocity of gliding reached approximately 20 μm/s.

I then analyzed the relationship between the two adjacent movements. Figs. 2-1c and 2-1d show measurements of the gliding of three and four cells, respectively. An oscillation period of the cell **A**/**B** pair is similar to that of the cell **B**/**C** pair in Fig. 2-1c, but phases of their oscillation are different. This is also somewhat true in the four-cell

measurement shown in Fig. 2-1d. It is likely that the delay in propagation of gliding oscillation from a pair of cells to the next may dictate overall movement of cells in a *B. paxillifer* colony.

2-3-2 Implication of two actin bundles positioned along a raphe in intercellular gliding of *B. paxillifer*

Previous studies in unicellular gliding diatoms indicate a pivotal role of actin filaments in their gliding motion. Therefore, I analyzed morphological characteristics of actin filaments in *B. paxillifer* cells by using fluorescence microscopy. When a single *B. paxillifer* cell stained with Alexa Fluor 488-labeled phalloidin was observed from the top (or bottom) of the cell, two actin bundles positioned on both sides of a raphe (Fig. 2-2a, arrow) were prominent (Fig. 2-2a). The two actin bundles appeared to be continuous, and no central discontinuity was seen. This corresponds to the fact that, in *B. paxillifer*, no central nodule exists so that a raphe of a valve is continuous from one end to the other. In the side view of a colony, two actin bundles, one located just near the top valve and the other near the bottom one, were observed in each cell, meaning that there were four actin bundles in a single *B. paxillifer* cell (Fig. 2-2b). The end of the actin bundles near the top and bottom valves curved along the edge of the valves; however, the top and bottom bundles did not seem to be connected. Appearance of these actin bundles is similar to that reported for other unicellular gliding diatoms, suggesting similar actin involvement in the gliding motion of *B. paxillifer*. I noted that all of the top and bottom actin bundles in all of the cells in a colony were observed in the same focal plane, indicating that these bundles are positioned precisely in a colony (Fig. 2-2b).

To examine whether the actin bundles observed adjacent to the raphe are indeed

involved in intercellular gliding of *B. paxillifer*, I examined the effects of latrunculin B, an actin-depolymerizing reagent, and BDM, a myosin inhibitor, on the gliding motion. A 5 μM final concentration of latrunculin B completely inhibited the gliding motion of *B. paxillifer* in less than 20 s (Fig. 2-3a). When latrunculin B was removed after an approximate 1-min treatment of the cells, their gliding motion resumed within 5 min. When the cells were incubated with latrunculin B for 30 min, their gliding motion was restored only after more than 12 h of incubation. The direction of gliding after restoration was not necessarily the same as that before inhibition. I also monitored the effect of latrunculin B on actin filaments in *B. paxillifer* by phalloidin staining. The actin bundles seen along the raphe disappeared completely after a 1-min treatment of *B. paxillifer* with 5 μM latrunculin B (Fig. 2-3b, middle panel), and the actin bundles reappeared within 5 min after removal of the drug under these conditions (Fig. 2-3b, bottom panel). These results indicate that the gliding is closely correlated with the existence of actin bundles along the raphe.

I then tested the effect of a myosin inhibitor, BDM. A 50 mM final concentration of BDM also inhibited the gliding of *B. paxillifer*, but BDM affected the gliding more slowly than did latrunculin B (Fig. 2-3c), taking nearly 5 min to stop the gliding completely. When BDM was removed after approximately 5 min of treatment of the cells, the gliding motion resumed within 1 min. The above results with latrunculin B and BDM implicate the actomyosin system in the gliding of *B. paxillifer*.

2-3-3 Ultrastructural analyses of the *B. paxillifer* cell surface

To help understand the gliding mechanism in *B. paxillifer*, I observed by SEM intracellular structures related to the cytoskeleton and cell surface structures connecting

two adjacent cells. When observed from the outside through the SEM, *B. paxillifer* cells were found to have one long raphe without a central nodule on each valve, as reported previously (Fig. 2-7a, arrow; Jahn and Schmid, 2007). To study intracellular structures that relate to the raphe and the cytoskeleton, I sonicated fixed *B. paxillifer* cells and observed hulls of the cells from the inside (Fig. 2-4a–4c). There is a long groove in the center of a cell hull, corresponding to the cell surface region of a raphe, and many arch-shaped structures called fibulae, which are perpendicular to the raphe, bridge both sides of this groove. A string-like structure with a diameter of ~270 nm was observed in this groove under the fibulae (Fig. 2-4b and 2-4c, arrowheads). Some regions of the string-like structure were divided into two by narrow spaces, which may suggest that the string-like structure consists of two closely aligned sub-strings (Fig. 2-4b, arrows). A magnified view shows that the string-like structure associated with one valve seems to terminate at the end of the valve (Fig. 2-4c).

In TEM, a longitudinal profile of a filamentous structure and cross-sections of fibulae was observed in a longitudinal section of *B. paxillifer* (Fig. 2-5). This filamentous structure (Fig. 2-5b, brackets) was located between a fibula (Fig. 2-5b, 'F') and a silicified cell wall (Fig. 2-5b, 'CW'). The width of the filamentous structure in this image is approximately 100 nm, and diameter of each filament within the structure is 5-7 nm. The end of the filamentous structure near the bottom valve curved along the edge of the valve (Fig. 2-5c, arrow), as expected from the SEM observation. The position of this filamentous structure is near the median line of a cell and similar to the position where the string-like structures were seen by SEM and where the actin bundles were observed by phalloidin staining.

It is noteworthy that electron-dense structures (Fig. 2-5a inset, arrowheads, and

2-5b, ‘D’) were observed between the filamentous structure and electron-lucent material outside the cell (Fig. 2-5b, ‘L’). The electron-dense structure underlies the membranous structure that is thought to be a plasma membrane (Fig. 2-5d, the lower arrow, and see also Fig. 2-6d). The electron-dense structures were seen along with the filamentous structures throughout the longitudinal section of the *B. paxillifer* cell, and they were interrupted by short gaps (Fig. 2-5a, inset, arrow). These electron-dense structures are approximately 25 to 35 nm in thickness and average 3 μm in length. On the other hand, the electron-lucent material (Fig. 2-5b, ‘L’, see also Fig. 2-6b, ‘L’) seems to fill the space between the plasma membrane and the silicified cell wall (Fig. 2-5b, see also Fig. 2-6b).

Cross-sections of *B. paxillifer* colonies revealed that one cell is connected to its adjacent cell through the raphe and that the raphe consists of a protrusion of the silicified wall with a narrow cavity opening to the interface of the opposing raphe protrusion (Fig. 2-6). A fibula passes through the cytoplasm and bridges both sides of the raphe (Fig. 2-6b, ‘F’). The space between a fibula and a part of the outer silicified cell wall (Fig. 2-6b, ‘CW’) is filled with aggregates of punctate structures that are approximately 6 to 9 nm in diameter (Fig. 2-6c), thought to be cross-sections of the filamentous structures observed in Fig. 2-5a and 2-5b. This region corresponding to the filamentous structures is continuous in the cross-section, and no apparent gap divides this region into two parts. Again, the electron-dense structure was observed between the plasma membrane and the filamentous structure (Fig. 2-6d, ‘D’). The dimensions of the cross-sectional shape of the electron-dense structure are approximately 350 nm for the long span and 20–50 nm for the short span (Fig. 2-6b, ‘D’, and 6e, arrows), but sometimes the structure was divided into two (Fig. 2-6e, a pair of arrows in the lower part). The electron-dense structure was not always observed in serial cross-sections, indicating discontinuity of this structure

along with the longitudinal axis of the cell (Fig. 2-6f and see Fig. 2-5a, inset, for the longitudinal section). In addition, electron-lucent material, which is thought to be mucilage, was observed in the raphe channel and in the extracellular space between the raphes of two adjacent cells (Fig. 2-6b, ‘L’ and 2-6e, ‘L’).

In summary, observations in both SEM and TEM revealed that the filamentous structure located between fibulae and the silicified cell wall, presumably an actin bundle, is aligned with the raphe and that there are discontinuous electron dense structures between the plasma membrane and the filamentous structure, also aligned with the raphe.

2-4 Discussion

I performed motion recordings and analysis of gliding and a morphological study of a colonial diatom, *B. paxillifer,* by both light and electron microscopy to help understand the molecular mechanism for its gliding. The light microscopic observations of living and fixed *B. paxillifer* cells revealed the following: (i) the gliding of two adjacent cell pairs in a colony is oscillatory and has a certain narrow range of oscillation periods, although the periods vary more among different colonies; (ii) inhibitors of the actomyosin system, namely latrunculin B and BDM, reversibly compromise the gliding; and (iii) the gliding is clearly correlated with the existence of two actin bundles along a raphe on a frustule. These results support the idea that the gliding motion of *B. paxillifer* cells is driven by the actomyosin system.

It has been proposed that gliding of unicellular pennate diatoms on the substratum, such as *Navicula cuspidate* and *Craspedostauros australis*, depends on actin filaments and an actin-binding protein that generates motive force along with the filaments, presumably myosin (Edgar and Pickett-Heaps, 1982; 1983; Edgar and Zavortink, 1983; Poulsen *et al*., 1999). Thus, the colonial diatom seems to use a similar motility system to drive intercellular gliding instead of gliding on the substratum. I noted that even a short (~20 s) treatment of latrunculin B is sufficient to stop the gliding and disassembles the actin bundles along the raphe completely, and that this inhibition is restored quickly by removing the drug. However, when *B. paxillifer* cells are treated for a longer period of time (~30 min) with latrunculin B, the effect is more deleterious and recovery from the drug requires a much longer period (~12 h) after drug removal. This may come from secondary perturbation of structures that are essential for gliding by the latrunculin B treatment, and maintenance of such structures may require some actin

cytoskeleton in *B. paxillifer* cells. Analysis of ultrastructural differences between the cells that received short latrunculin B treatment and those that received long treatment might reveal such putative structures required for gliding (see below).

Previous reports showed that myosin runs on actin filaments at a rather constant velocity in *in vitro* motility assays (e.g., Umemoto and Sellers, 1990). This is in contrast to the gradual change of gliding velocity in *B. paxillifer* insofar as the velocity of the gliding motion of a pair of cells usually reaches a maximum when tip distance between the two adjacent cells nears zero, whereas the velocity becomes zero when the cells are in the most extended configuration in the colony. If the gliding motion is driven by the actomyosin system then the motor system should be equipped with some mechanism to achieve this oscillatory movement. Harper and Harper (1967) reported an elasticity of the mucilage that is secreted from the raphe by quantitative analysis of cell adhesion to the substratum in a unicellular gliding diatom. Such elastic materials linking putative gliding motor units and the cell body might act as springs to enable this kind of movement.

In addition, the gliding of diatoms is generally bi-directional. Although the mechanism underlying this bi-directionality is still unknown, it is proposed that the presence of two actin bundles plays a pivotal role. One possibility is that two actin bundles have a different polarity and that myosin motors change their moving track from one actin bundle to the other during the change in direction. An alternative possibility is that two actin bundles have the same polarity and that multiple classes of myosins are involved—a conventional barbed-end directed myosin and an atypical pointed-end directed myosin, such as myosin VI (Wells *et al*., 1999). Thus, determination of polarity of the actin bundles will help resolve this ambiguity.

On the other hand, SEM observations of *B. paxillifer* cells provided clues

regarding ultrastructural entities involved in gliding. String-like structures were observed in the groove along the raphe, and they were positioned between the fibulae and the silicified cell wall. TEM analysis indicated that, in the longitudinal sections of *B. paxillifer* cells, structures consisting of fine filaments were aligned in the space between the fibulae and the cell wall, and in the cross-sections, punctate structures with diameters of approximately 6–9 nm occupy the space surrounded by the fibulae and the cell wall near the raphe. Because distribution of the string-like structure in SEM and that of the filamentous structures in TEM are quite similar to that of actin bundles observed in phalloidin staining under the fluorescence microscope, I conclude that these structures correspond to the actin bundles. The actin bundle mostly appears as a single entity along the raphe in both SEM and TEM images, which is not consistent with the double-bundle appearance in phalloidin staining. This may be an artifact of bundle coalescence induced by the drying process needed for EM sample preparation. Because the two actin bundles are held in a narrow space by the fibulae and the outer silicified cell wall, close apposition of the two bundles may cause such an artifact. Indeed, similar observations, two actin bundles located along raphe, were also reported previously in the unicellular gliding diatoms *N. cuspidate* and *C. australis* (Edgar and Pickett-Heaps, 1982; 1983; Edgar and Zavortink, 1983; Poulsen *et al*., 1999).

The SEM and TEM observations have revealed another novel structure that might be involved in gliding. The electron-dense structures were observed by TEM; these structures are aligned intermittently along the raphe and the actin bundles. These structures might link the actin filaments with the plasma membrane. Because the driving force generated through the actomyosin system inside the cell needs to be transmitted to the cell surface, and because structures involved in this power transmission should have

enough strength and rigidity to allow movement of a cell, such structures should be observed by TEM as protein-rich regions (*i.e.*, regions with a certain electron density). To my knowledge, the electron-dense structures described here have not been reported previously in other pennate diatoms. Thus, these are the primary candidates for the next stage of analysis; thus, I am interested in examining the structural changes during actomyosin inhibitor treatment, especially during prolonged exposure of *B. paxillifer* cells to latrunculin B as mentioned before.

The electron-lucent material was observed at the intercellular connection, the raphe channel, and the space between the cell wall and the plasma membrane with which the electron-dense structures are associated. It was assumed that the mucilage, which unicellular gliding diatoms secrete from the raphe, was used as a connector between the cell body and the substratum. Indeed, this electron lucent material seems to be only the structure existing between and connecting the two adjacent *B. paxillifer* cells. Thus, it may have some role in the gliding motion.

2-5 Figures

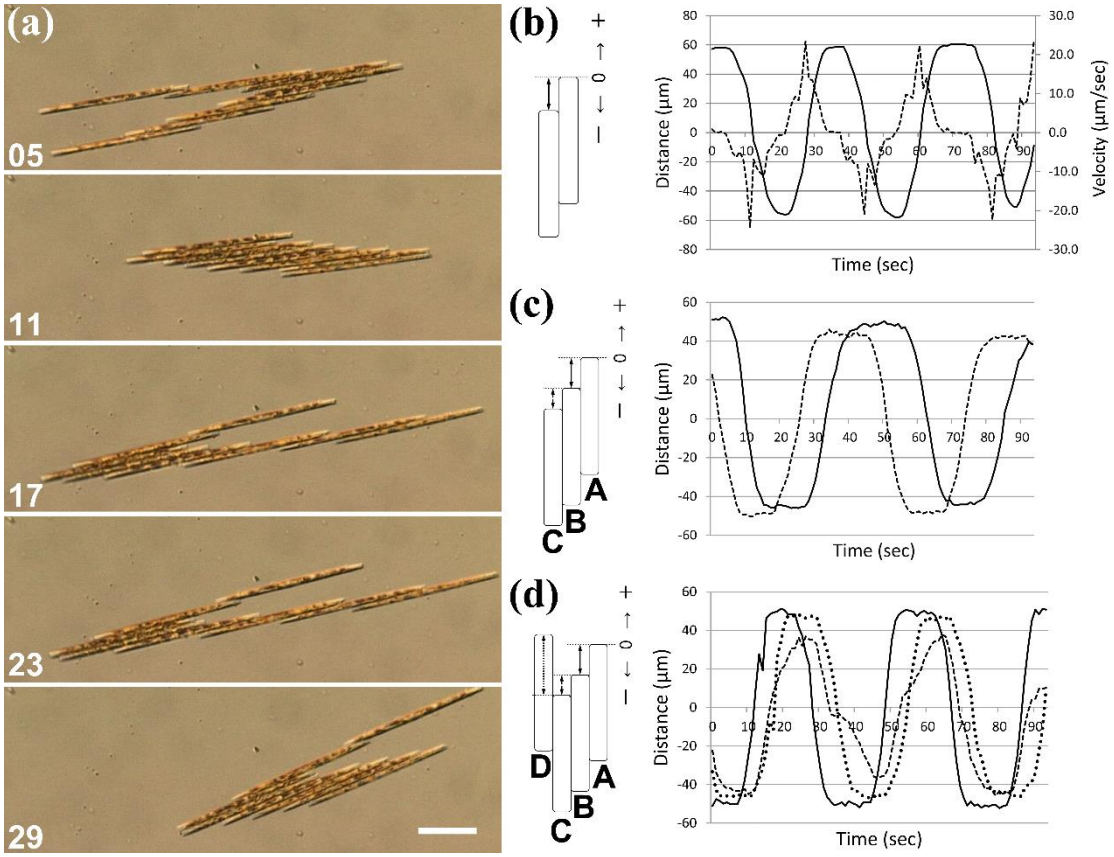

Fig. 2-1. Quantitative analysis of gliding motion of *B. paxillifer* cells. (a) Typical gliding of a *B. paxillifer* colony is shown in the series of time-lapse micrographs. A colony in ASW was observed under the brightfield, and the movement of the cells was recorded at the video rate. Time-lapse images at intervals of 6 s were shown. Duration after the beginning of recording is indicated on the lower-left corner. Bar = 50 μm. (b) A schematic drawing and quantitative analysis of gliding of two adjacent cells in a *B. paxillifer* colony. The ordinate, distance between tips of the adjacent cells (in micrometers); the abscissa, time (in seconds). The distance between tips of the two adjacent cells (continuous line) is measured as the length parallel to the longitudinal axis of the cells. The relative velocity is plotted with broken line. (c) Similar measurements were done with a three-cell colony, and the distance between the two adjacent cells is plotted as in (b). The distance between

cell **A** and cell **B** is shown in continuous line, and that between cell **B** and cell **C** is in broken line. (d) A four-cell colony is subjected to the similar analysis as in (c). The distance between cell **A** and cell **B**, that between cell **B** and cell **C**, and that between cell **C** and cell **D** are shown in continuous, broken and dotted lines, respectively.

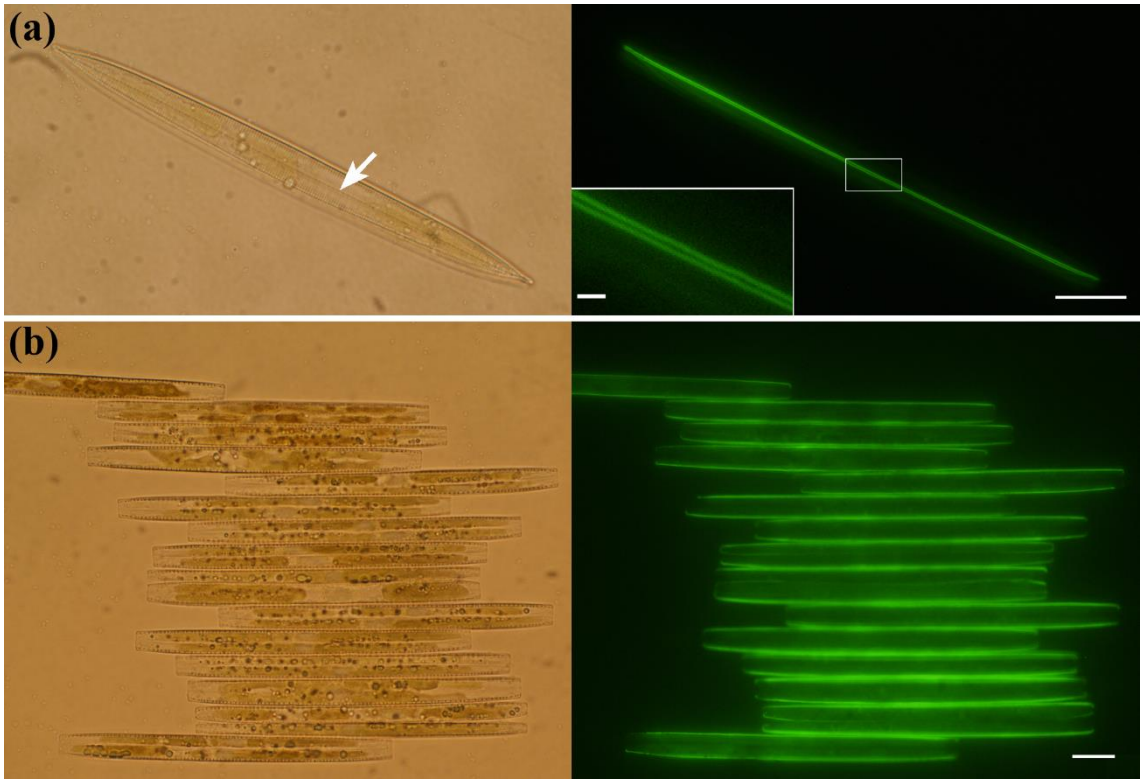

Fig. 2-2. Alexa Fluor 488-labeled phalloidin staining of *B. paxillifer*. (a) A top view of a single cell, viewed under the brightfield microscope (left) and under fluorescence observation (right). Prominent linear staining along the raphe is observed. An arrow points to the raphe. Bar = 10 μm. The inset of the right panel is a magnified view of the boxed region. Bar = 1 μm. (b) A side view of a colony, observed under the brightfield (left) or under fluorescence observation (right). Prominent staining of actin bundles in a colony is generally observed in a single focal plane. Bar = 10 μm.

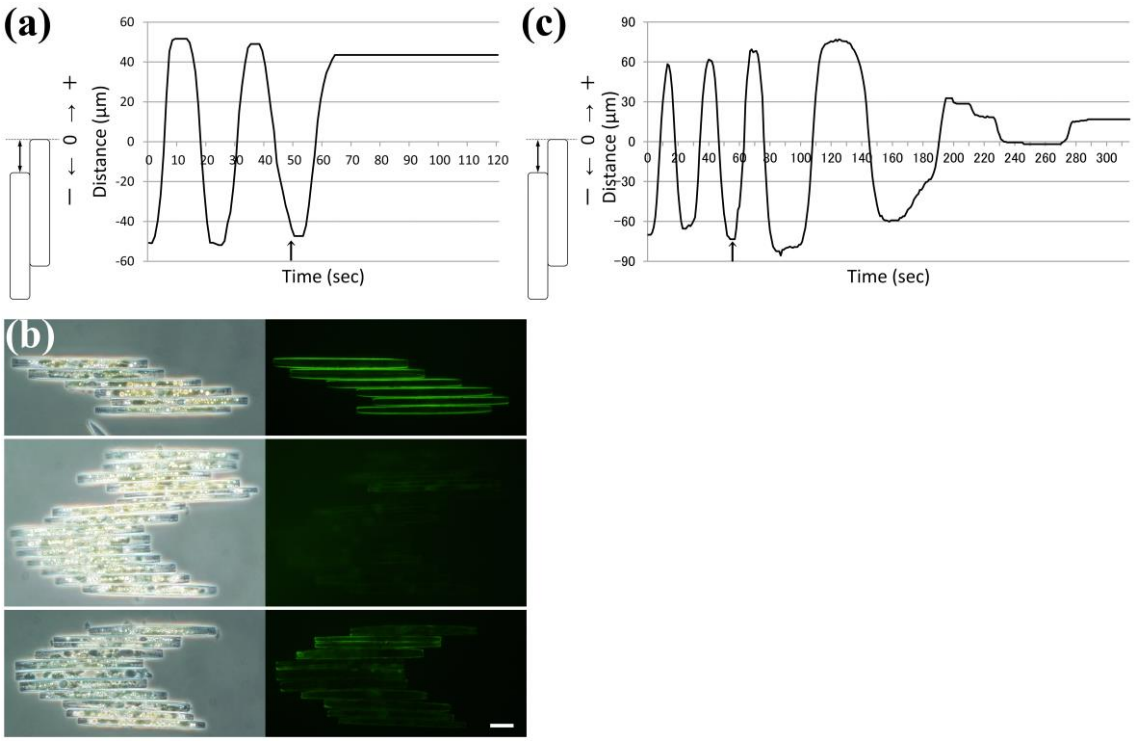

Fig. 2-3. Inhibition of gliding motion with actomyosin-related inhibitors. (a) A schematic drawing and quantitative analysis of gliding motion of two adjacent cells in an experiment with latrunculin B. The graph represents distance between tips of the two adjacent cells (see schematic drawing) as a function of time. The medium surrounding *B. paxillifer* cells was replaced with the medium containing final 5 μM latrunculin B at the time point of 48 s (arrow). (b) Phalloidin staining of latrunculin B-treated cells. A pair of two images consists of a phase contrast image (left) and a fluorescence image from Alexa Fluor 488-labeled phalloidin (right). The top row shows a colony before latrunculin B treatment. The middle row shows a colony treated with 5 μM latrunculin for 1 min. The bottom row shows a colony treated with latrunculin B for 1 min and then rinsed with ASW to remove the inhibitor. The images were taken after 5 min of the rinse. Bar = 20 μm. (c) A schematic drawing and quantitative analysis of gliding motion of two adjacent cells in an experiment with BDM are shown. The medium surrounding *B. paxillifer* cells

was replaced with the medium containing final 50 mM BDM at the time point of 54 s (arrow).

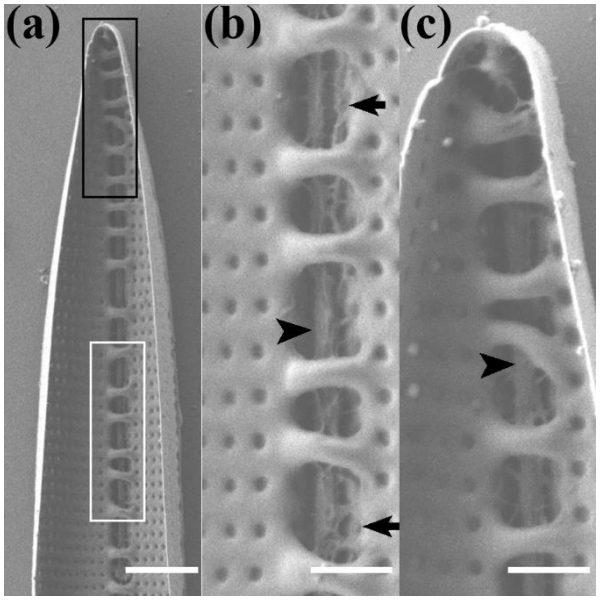

Fig. 2-4. SEM analyses of *B. paxillifer*. (a–c) Inside views of a fractured cell observed by SEM. (b) A magnified view of the region boxed with white line in (a). An arrowhead points the string-like structure. Arrows point to regions of the string-like structure, where it appears as two parallel strings separated by a narrow space. (c) A magnified view of the region boxed with black line in (a). An arrowhead points to the string-like structure. Bars = 3 μm for (a), and 1 μm for (b) and (c).

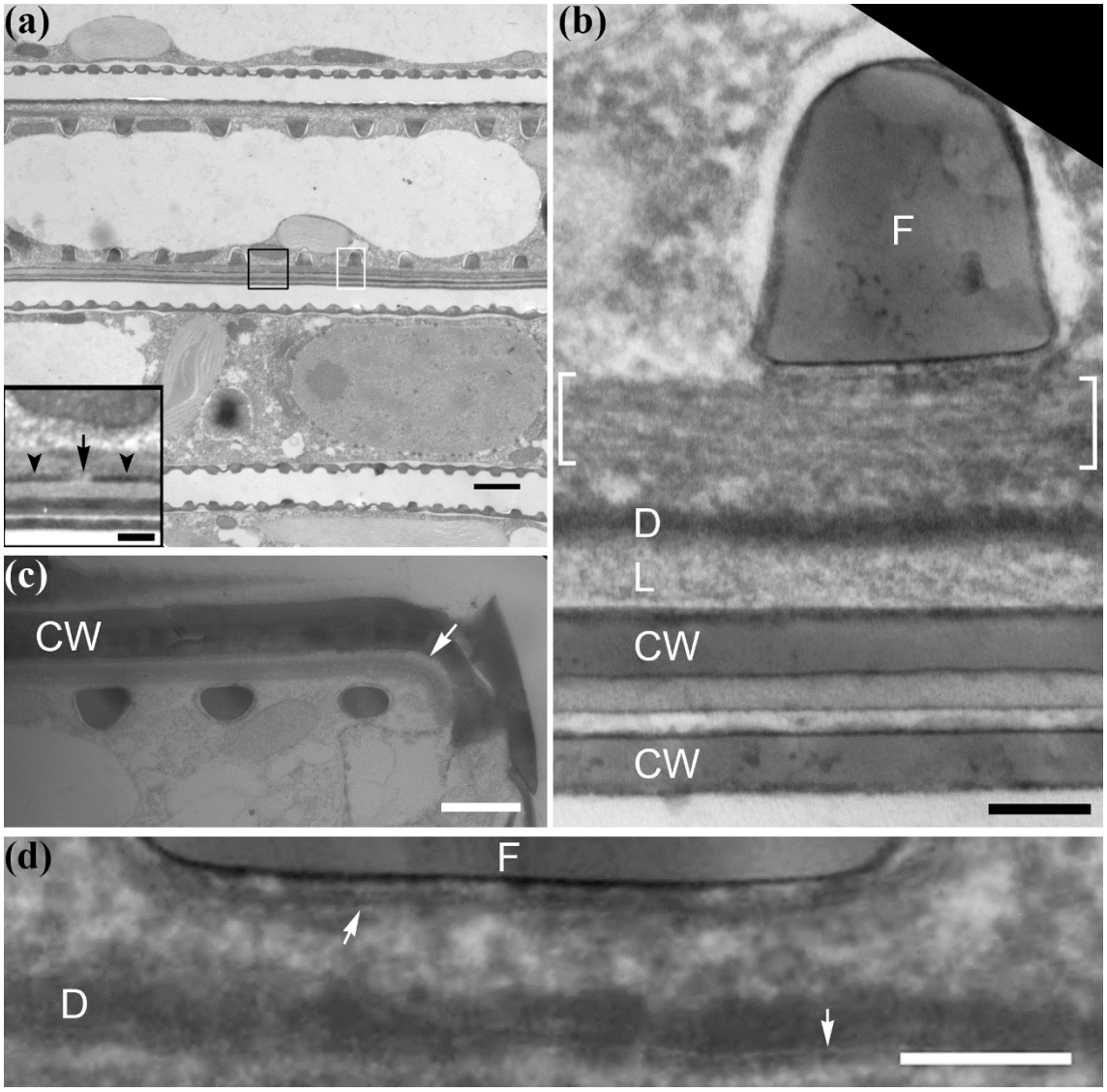

Fig. 2-5. TEM analyses of longitudinal sections of *B. paxillifer*. (a) A longitudinal section of a *B. paxillifer* cell, passing the median line of the cell observed by TEM. Bar = 1 μm. Inset is a magnified view of the region boxed with black line. An arrow points to a gap of the electron dense structures along with the filamentous structure. Bar = 200 nm. (b) A magnified view of a region boxed with white line in (a). A region marked with 'F' is a cross-section of a fibula. The area marked with brackets corresponds to a filamentous structure present between the fibula and the outer silica wall (CW) and discussed in the text. Layers marked 'D' and 'L' correspond to the electron dense

structure, and the electron lucent material, respectively. Bar = 100 nm. (c) A longitudinal section of a tip of *B. paxillifer* cell in other sample. An arrow points to the filamentous structure curved along with the edge of the valve. The region marked with 'CW' corresponds to the outer silicified cell wall. Bar = 500 nm. (d) A magnified image of a region between a fibula and an electron dense structure. 'D' and 'F' indicate as in (b). Arrows point to the structures that resemble the plasma membrane. Bar = 100 nm.

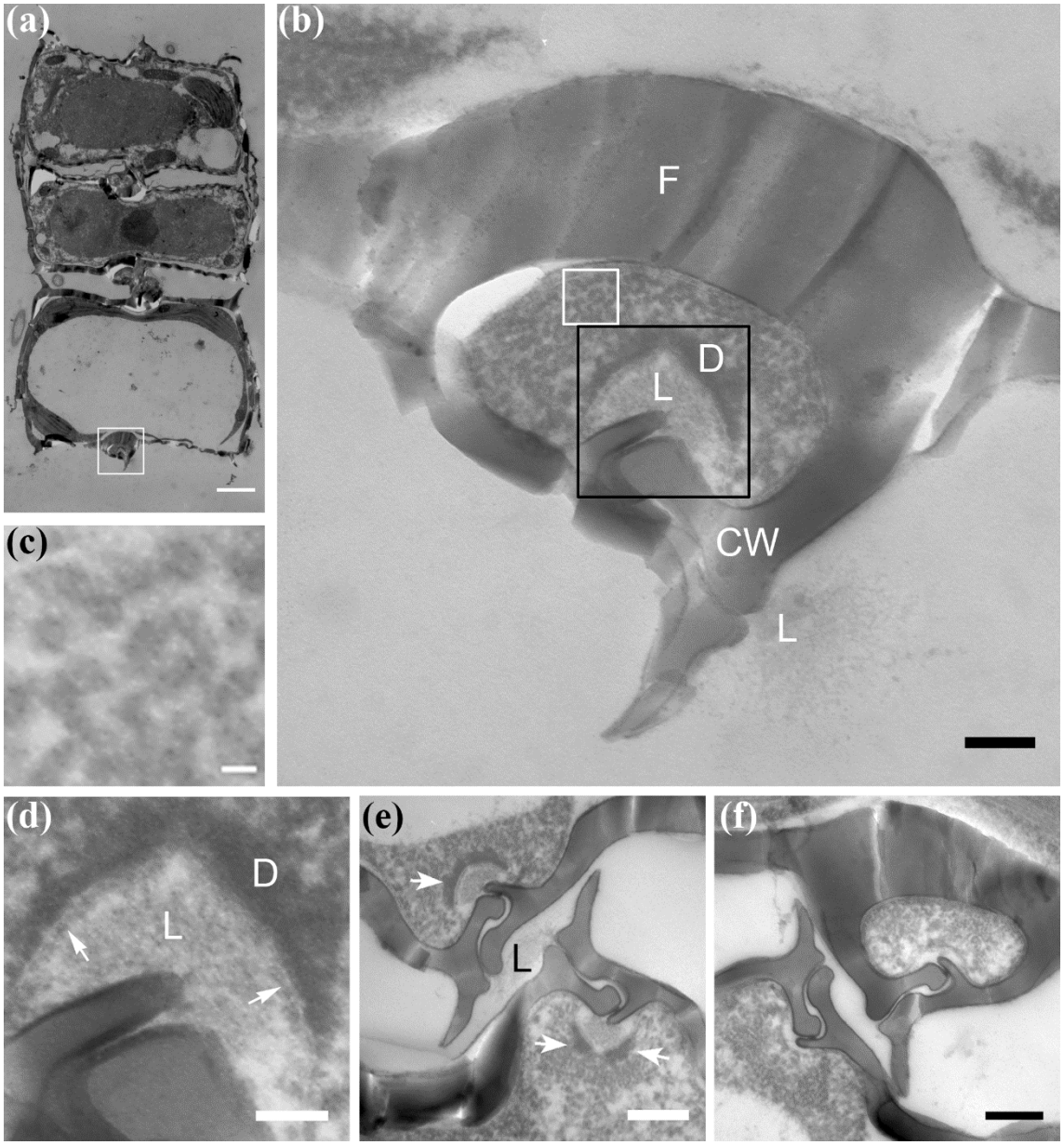

Fig. 2-6. TEM analyses of cross-sections of *B. paxillifer*. (a) A cross-section of three adjacent *B. paxillifer* cells. Bar = 1 μm. (b) A magnified view of the region boxed in (a). The punctate structures occupy the space between the fibula and the outer silica wall. Marking with 'F', 'D', 'L' and 'CW' is done as in Fig. 2-5. Bar = 100 nm. (c) A magnified view of the region boxed with white line in (b). Bar = 10 nm. (d) A magnified view of the region boxed with black line in (b). 'D', 'L' and 'CW' indicate as in Fig. 2-5. Arrows point to the structure that resembles the plasma membrane. Bar = 50 nm. (e) and (f) The

magnified cross-section, including interface of two adjacent cells in other samples. Arrows indicate the electron dense structures. Bars = 200 nm.

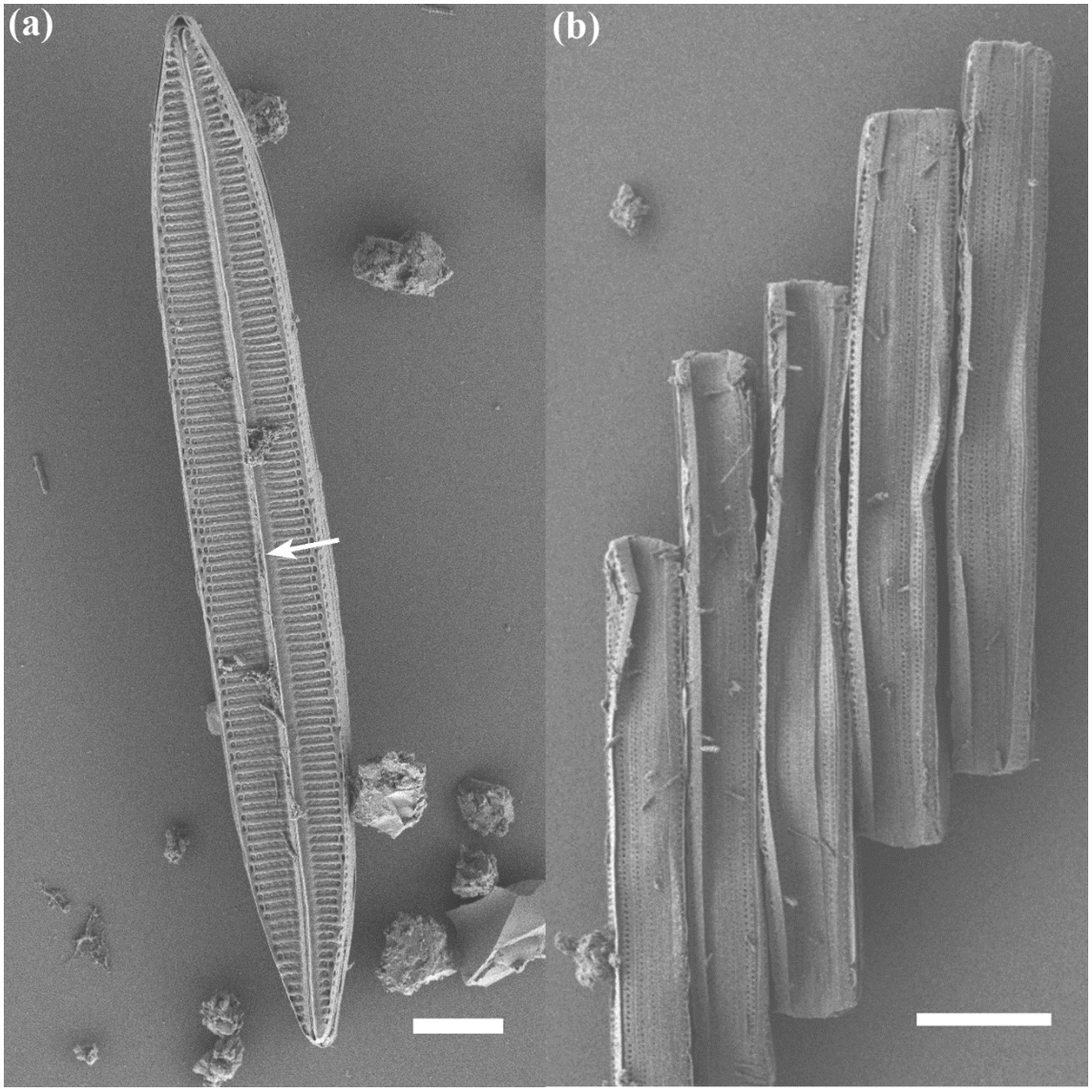

Fig. 2-7. SEM images of a whole cell and a colony. (a) A top view of a *B. paxillifer* cell. An arrow points to one straight raphe on the center of the valve. Bar = 5 μm. (b) A side view of a colony. Adjacent cells are always connected through the cell wall surfaces via the raphe. Bar = 10 μm.

Chapter 3

Gliding mechanism of the unicellular diatom,

Pleurosigma sp.

3-1 Introduction

Although some unicellular pennate diatoms generate power for gliding on the substratum, the molecular mechanism of this motion is not understood well. Edgar and Pickett-Heaps (1984) proposed a hypothesis for the gliding motion based on ultrastructural observations and actin distribution: Power for the gliding motion is generated by intracellular actin filaments located along the raphe and motor proteins associated with the actin filaments. The motive force generated by the actin and motor proteins is transmitted to the cell exterior through a putative transmembrane protein that links the motor proteins and the mucilage connecting the cell surface to the substratum (Edgar and Pickett-Heaps, 1984; Wetherbee *et al*., 1998). Inhibition of the gliding with inhibitors for actin and myosin supported involvement of the actomyosin system in gliding, but there was no biochemical information about these molecules (Poulsen *et al*., 1999).

Various putative myosins were annotated in the whole-genome projects of the centric diatom *Thalassiosira pseudonana* and the pennate diatom *Phaeodactylum tricornutum* (Montsant *et al*., 2007; Heintzelman and Enriquez, 2010). Gliding motion has apparently never been observed in *T. pseudonana*, but predicted myosin sequences suggested that *T. pseudonana* myosins belong to class XXII, XXIII and XXIV, the class of chromalveolate myosin (De Martino *et al*., 2007; Foth *et al*., 2006). On the other hand, gliding motion of *P. tricornutum* is observed in its oval state, which is induced by stresses, such as cold or low salt, they don't glide normally (Lewin *et al*., 1958; Lewin, 1958). In addition, the oval state don't have any silica cell wall, thought the gliding motion of the oval state is different from the other gliding diatoms do. Ten myosins were predicted from the genome sequence, but it remains to be addressed which myosin homolog is

responsible for the gliding motion (Heintzelman and Enriquez, 2010).

Diatom gliding is thought to be based on a unique mechanism, that is, an interior motor protein moves the exterior mucilage. To understand molecular mechanism of the gliding, biochemical identification and analysis of the motor protein are indispensable. So I tried to identify a motor protein(s) from unicellular gliding diatom, *Pleurosigma* sp. and found a candidate as the 130 kDa actin-binding protein.

3-2 Materials and Methods

Cell culture

Pleurosigma sp. was isolated from the sea coast in Yonago City, Japan. Cells were cultured in Daigo's Artificial Seawater SP (Nihon Pharmaceutical, Tokyo, Japan) supplemented with Daigo's IMK Medium (Nihon Pharmaceutical) and Na_2SiO_3 (Wako, Osaka, Japan) as a source of silicate. The culture was maintained at 25°C under an 18-h light/6-h dark cycle with light supplied by fluorescent lamps at 9.4 μmol/(m^2 s). For mass culturing, cells were cultured in artificial seawater, Marin Art SF-1 (ASW; Tomita Pharmaceutical Co., Tokushima, Japan) supplemented with IMK Medium and Na_2SiO_3 in shallow polystyrene boxes. The culture was kept near the window on the north side of the laboratory at room temperature throughout the year.

Preparation of crude extract

Two to three grams of cells were collected by filtration through a nylon filter having a passage aperture of 30 μm (Nippon Rikagaku Kikai Co., Tokyo, Japan) and rinsed in ice-cold EMP (50 mM PIPES-KOH, pH 7.0, 5 mM EGTA, 2 mM $MgCl_2$, 1 mM DTT, 0.4 mM phenylmethylsulfonyl fluoride (PMSF) and a proteinase inhibitor mixture (PI) containing 20 μg/mL leupeptin and 20 μ/mL pepstatin A). Cells were collected by centrifugation at 140 ×g for 2 min (LC-1000; TOMY, Tokyo, Japan), rinsed in 20 mL of EMP, and mixed with 8 mL of soda-lime silicate glass beads of 400 μm in diameter (UB-1315L; UNITIKA, Tokyo, Japan) for 2 min using automatic lab mixer HM-10 (AS ONE, Osaka, Japan) in the cold room. Material including open frustules were collected by centrifugation at 850 ×g for 2 min, and the supernatant was discarded. The precipitate was washed with 5 mL of EMP for three times, incubated with 10 mL of ice-cold

extraction solution containing 1 M NaCl, and then settled on ice for 15 min. The sample was centrifuged at 850 ×g for 2 min to remove the frustules, and the supernatant was further centrifuged at 290,000 ×g for 10 min (Himac CS 120GX; Hitachi, Tokyo, Japan) at 2°C. The supernatant was concentrated and desalted by a Vivaspin 20 concentrator (50,000 MWCO, Sartorius Stedim Biotech, Goettingen, Germany) at 5,000 ×g (Himac CR 2LG: Hitachi) at 2°C until concentration became satisfactory to yield a crude extract subjected to the following analyses.

Purification of a 130 kDa polypeptide

Chicken skeletal muscle actin was isolated from acetone-dried muscle powder and purified according to the method of Spudich and Watt (1971). Chicken skeletal muscle actin (50 μg) was added to the crude extract fraction (0.5 mL), incubated for 5 min at room temperature and mixture was centrifuged at 368,000 ×g for 10 min at 2°C. The precipitate was resuspended in 50 μL of EMP supplemented with 2 mM ATP and 0.5 M KCl and incubated for 5 min at room temperature. After centrifugation at 368,000 ×g for 10 min at 2°C, the supernatant was collected as an actin-associated fraction.

***In vitro* motility assay**

An *in vitro* motility assay was performed according to Warshaw *et al*. (1990). In brief, the motor fraction containing the 130 kDa polypeptide was spread on a coverslip pre-coated with 0.1% v/v collodion (Nisshin EM, Tokyo, Japan) in 3-methlybutyl acetate (Wako). The rhodamine phalloidin-labeled chicken skeletal muscle actin (20 μL of 0.25 μg/mL solution containing 0.1 mg/mL glucoseoxidase, 0.02 mg/mL catalase, 10 mg/mL glucose and 5 mg/mL methyl cellulose #400) was perfused to the coverslip with 2 mM

ATP. The prepared specimen was warmed up at the expiration and observed under a fluorescence microscope at room temperature.

Preparation of a monoclonal antibody against the 130 kDa polypeptide

Monoclonal antibodies were prepared using standard methods. In brief, the actin-associated fraction with a total of ~50 μg protein was injected into eight-week-old female mice (BALB/cAJc1; CLEA Japan, Inc., Tokyo, Japan). Thirty six days later, spleen cells were isolated from the immunized mice, fused with myeloma (P3×63-Ag.8.653) using 50% w/v polyethylene glycol (PEG) 1500 in 75 mM Hepes, and incubated in a CO_2 incubator (ASTEC, Fukuoka, Japan) to establish hybridoma clones. Hybridoma clones were multiplied in HAT medium selectively and the screening was performed by ELISA method. Finally, 19 clones of hybridoma producing antibodies recognizing the 130 kDa polypeptide, and 4 clones recognizing the 45 kDa polypeptide were obtained.

Fluorescence microscopy

For phalloidin staining, cells were fixed with 3.6% w/v formaldehyde in phosphate-buffered saline (PBS) for 60 min, permeabilized with 0.02% w/v Triton X-100 in PBS, and stained with 33 nM Alexa Fluor 488-labeled phalloidin (Invitrogen, Carlsbad, CA, USA) at room temperature. Samples were observed with an epifluorescence microscope, BX-50 (Olympus, Tokyo, Japan), equipped with a CCD camera, DP70 (Olympus).

For immuno-staining, cells were fixed with 3.6% w/v formaldehyde in PBS for 60 min, crushed with soda-lime silica glass beads of 400 μm in diameter, incubated with the primary antibody for 1 hr at room temperature, rinsed in PBS three times, and then

incubated with the secondary antibodies, Alexa Fluor 488-labeled goat anti-mouse IgG (H+L) (Invitrogen), for 1 hr at room temperature. Samples were observed with an epifluorescence microscope, BX-50 (Olympus, Tokyo, Japan), equipped with a CCD camera, DP70 (Olympus).

Analysis of amino-acid sequence

Because it was found that the N-terminus of the 130 kDa polypeptide was blocked, the Cleveland procedure (Cleveland, *et al*., 1977) was used to obtain the peptide fragments. In brief, the desired band was cut out from an SDS-polyacrylamide gel, rinsed with 100% methanol (Wako) for 10 min, and rehydrated with SDS-PAGE sample buffer. The rehydrated band was set into a well of a 15% polyacrylamide gel having a long stacking gel, followed by 10 μL of SDS-PAGE sample buffer and 10 μL of V8 protease solution (500 μg/mL V8-protease in 125 mM Tris-HCL, pH 6.8, and 1 mM EDTA) (Sigma-Aldrich, St. Louis, MO, USA), and then electrophoresed. The electrophoresis was suspended for 30 min when all the proteins entered the stacking gel to digest the polypeptide with V8 protease, and then restarted. The digested polypeptides were transferred to a polyvinylidene difluoride (PVDF) membrane (Bio-Rad Laboratories, Inc. Hercules, CA, USA), and each band separated from the membrane sheet was subjected to N-terminal amino acid sequencing using a protein sequencer, ABI Procise 494HT and 492cLC (Applied Biosystems, Carlsbad, CA, USA), by pulsed-liquid or gas-phase methods. The amino acid sequencing was performed by Dr. Y. Makino in National Institute for Basic Biology. The sequences were subjected to homology search with the FASTA program.

3-3 Results

3-3-1 Actin localization of a unicellular diatom, *Pleurosigma* sp.

Previous studies in unicellular diatoms reported existence of actin bundles along the raphe, and suggested a pivotal role of actin bundles in gliding motion of diatoms. Therefore, I investigated the morphological characteristics of actin filaments in *Pleurosigma* sp. cells with the fluorescence microscope. Two actin bundles positioned on both sides of a raphe were prominent when *Pleurosigma* sp. cells stained with Alexa Fluor 488-labeled phalloidin were observed from the top of cells (Fig. 3-1a). The two actin bundles are continuous from one end of the cell to the other, and are not interrupted by the central nodule (Fig. 3-1a, arrowhead). In the side view of cells, the two actin bundles are found just beneath each valve, and each bundle is bent in the middle where the central nodule exists (Fig. 3-1b). The upper and lower actin bundles appear to be independent, and were never seen to be fused at the cell tip. The appearance of the actin bundles is similar to that reported previously in other unicellular diatoms (Edgar and Zavortink, 1983; Poulsen *et al*., 1999), suggesting that such actin organization is common to pennate diatoms.

3-3-2 Isolation of a 130 kDa polypeptide

Several reports suggest that actin is involved in gliding motion of diatoms and that motor a protein acting on actin, presumably myosin, drives the motion (Edgar and Pickett-Heaps, 1983; 1984; Edgar and Zavortink, 1983; Poulsen *et al*., 1999). The candidates for myosin were predicted from whole-genome sequence analysis of *T. pseudonana* and *P. tricornutum*, but biochemical characterization has apparently never been reported. Therefore, I searched for candidate motor proteins involved in the gliding

in *Pleurosigma* sp. biochemically.

In the putative gliding machinery, motor proteins are presumed to be associated both with actin bundles along the raphe and with putative transmembrane proteins inserted in the cell membrane. So, I reasoned that the gliding machinery is associated with the inner surface of the cell membrane captured on the valve even after diatom cells are disrupted by harsh agitation with glass beads, and washed with buffer to remove the cytoplasm. Fig. 3-2 shows examples of the diatom cells before and after disruption by bead agitation. From the SEM observation, sets of two valves fittiing each other were observed in a sample of intact cells, while independent but intact valves were prominent after cell disruption (Fig. 3-2a). To investigate morphology of actin filaments, the samples before and after the cell disruption were stained with Alexa Fluor 488-labeled phalloidin and observed through the microscope (Fig. 3-2b). Before cell disruption, the two actin bundles along the raphe and chloroplasts were seen (Fig. 3-2b, left panels). On the other hand, after agitation, some chloroplasts were released from cell hulls but the two actin bundles were almost intact (Fig. 3-2b, middle panels). Almost all the chloroplasts and a large part of the actin bundles were removed from the cell hulls by washing with buffer (Fig. 3-2b, right panels). I supposed that the gliding machinery remained on the hulls (i.e., was not removed by the buffer wash) by virtue of its strong interaction with the cell membrane components. Thus, the fraction containing the cell hulls was subjected to further analyses.

A salt extract was prepared from the cell hull fraction with 1.0 M NaCl, and the supernatant was used as an initial material for purification (hereafter named as “crude fraction”). I reasoned that, if motor proteins generating moving force along actin filaments are released from diatom’s actin bundles on the cell hulls, such proteins can be

re-captured by binding filamentous-actin and be isolated by appropriate centrifugation. Indeed, when I mixed the crude fraction with chicken skeletal muscle filamentous actin, a 130 kDa polypeptide was co-precipitated as the most prominent band. This association was specific since interaction between the 130 kDa polypeptide and actin was partially inhibited by adding 2 mM ATP (Fig. 3-3a). Thus, the 130 kDa polypeptide seemed to bind actin in an ATP-sensitive manner.

Purification of the 130 kDa polypeptide was carried out using these properties. While the 130 kDa polypeptide is co-precipitated with the chicken filamentous actin almost quantitatively, its release from the co-precipitated actin in the solution containing ATP was insufficient. By searching for preferable conditions to release the 130 kDa polypeptide from actin, I found that incubation of the co-precipitate with buffer containing both 2 mM ATP and 0.5 M NaCl was the most efficient so far. The solution containing either ATP or NaCl alone released the 130 kDa polypeptide poorly from the co-precipitate (Fig. 3-3b). Using these conditions, I partially purified the 130 kDa protein with relatively few contaminants.

3-3-3 Characterization of the 130 kDa actin-binding polypeptide

I examined whether this 130 kDa actin-binding polypeptide is related to myosin, and also investigated a possibility that the polypeptide works as a motor in the gliding motion of the diatom. One of the most significant features of myosin is to move on the actin filament, and this can be tested by the *in vitro* motility assay. In the *in vitro* motility assay, a glass slide coated with proteins in question was incubated with fluorescent-labeled chicken skeletal muscle actin filaments, and movement of the filaments was monitored under the microscope. Indeed, the crude fraction containing the 130 kDa

polypeptide could drive the movement of fluorescent actin filaments, suggesting that the crude fraction contains myosin-like motor activities (Fig. 3-4). The velocity of actin movement observed in the assay was 2.8 μm/s on average, which is at the lower end of the range of gliding velocity observed in cells (1 to 25 μm/s depending upon conditions; Edgar, 1979; Round *et al*., 1990; Gupta and Agrawal, 2007). Unfortunately, the purified fraction could not drive the movement of the fluorescent actin filaments, perhaps because of irreversible inactivation of motor proteins upon /high salt extraction.

Next, I tried to obtain structural information about the 130 kDa polypeptide. First, the 130 kDa polypeptide was subjected to N-terminal sequencing, but its N-terminus was evidently blocked. Then, I tried to obtain internal sequences. The 130 kDa polypeptide was hydrolyzed with V8 protease which cleaves peptide bonds at the carboxylic side of glutamate and aspartate residues, and the resulting peptides were sequenced, yielding one amino acid sequence: ELIESRTGLCAMLNEECVRP. This amino acid sequence has a similarity to myosin from another pennate diatom, *P. tricomutum,* whose genomic sequence was reported previously (Fig. 3-5a and 3-5b; Heintzelman and Enriquez, 2010). The obtained partial sequence has more than 70% identity and 90% similarity to *P. tricomutum* myosins A, C, E, and G (PtMyoA, C, E and G) although the available sequence information from the *Pleurostigma* protein was limited. Thus, it is possible that the 130 kDa polypeptide is related to myosin from its molecular weight, actin-binding properties, and partial amino sequence.

I then investigated localization of the 130 kDa polypeptide. For this and other purposes, I raised mouse monoclonal antibodies against the 130 kDa polypeptide. Because some low molecular weight bands were seen in the final 130 kDa polypeptide fraction, and I was still on the way to complete purification of the 130 kDa polypeptide,

it was more advantageous to obtain monoclonal antibodies than raising polyclonal antibodies. Indeed, I obtained several lines of hybridoma expressing antibodies specifically recognizing the 130 kDa band on western blots. Immuno-fluorescence microscopy of fixed and disrupted *Pleurosigma* sp. cells with one of the anti-130 kDa polypeptide antibodies demonstrated that the 130 kDa polypeptide is localized on a set of two adjacent lines. The staining of the line was sometimes punctate but at other times was continuous. The 130 kDa polypeptide staining appeared to be on he two parallel actin bundles beside the raphe (Fig. 3-6a). Similar localization was also observed near the raphe, even in specimens without detectable actin bundles remaining (Fig. 3-6a and 3-6b, arrows). From these results, I propose that the 130 kDa actin-binding polypeptide is a myosin-like motor that contributes to the gliding motion in the unicellular diatom.

3-4 Discussion

I tried to identify the motor protein from the unicellular gliding diatom, *Pleurosigma* sp. to help understand the molecular mechanism of its gliding motion, and succeeded in isolating a 130 kDa polypeptide that co-precipitated with chicken skeletal muscle actin. Biochemical experiments revealed that the 130 kDa polypeptide has myosin-like features: (i) partial amino acid sequence of the 130 kDa polypeptide has a high similarity to annotated myosins in the *P. tricomutum* genome, (ii) the crude fraction containing the 130 kDa polypeptide could drive actin-filament movement in the *in vitro* motility assay and, (iii) immunofluorescence microscopy with an anti-130 kDa polypeptide antibody demonstrated its localization along the raphe. These results suggested that the 130 kDa polypeptide is a myosin-like-protein and a candidate of motor protein responsible for the gliding motion in *Pleurosigma* sp.

Previous studies, using inhibitors for actin and myosin, presumed the involvement of myosin as a motor protein in the gliding motion, that is, in the gliding machinery. The motor protein was suggested to interact with both actin bundles along the raphe and putative transmembrane protein embedded in the cell membrane, and force generated by actomyosin is transferred to mucilage in the cell exterior (Poulsen *et al*., 1999). *Pleurosigma* sp. also has a pair of actin bundles along the each raphe, and the center of bundles bend at the central nodule. Such appearances and localization are similar to those of other unicellular diatoms, *Navicula cuspidate* and *Craspedostauros australis,* and are consistent with the idea that *Pleurosigma* sp. uses actin filaments to drive the gliding motion on the substratum (Edgar and Zavortink, 1983; Poulsen *et al*., 1999).

Through sequencing, *P*. *tricornutum* was annotated as having ten myosin orthologues in its genome (Heintzelman and Enriquez, 2010), but there is little if any

information about their biological functions. The partial amino acid sequence of the 130 kDa polypeptide has a similarity with some of these myosins, that is: PtMyoA, C, E, and G. This sequence, conserved among these four *P. tricornutum* myosins, is in the middle part of the head domain. The 130 kDa polypeptide also has a similar molecular mass with these myosins. The partial sequence also has 64% identity with similar sequences of the head domain of a myosin-Ib-like protein from the Chinese hamster, *Cricetululus griseus*. Thus, these similarities in the partial amino acid sequences support the possibility that the 130 kDa polypeptide belongs to the myosin family.

In the *in vitro* motility assay, the crude fraction containing the 130 kDa polypeptide drove the movement of actin filaments, suggesting that the crude fraction indeed contained a myosin-like motor activity to drive actin movement, but it was not confirmed whether the 130 kDa polypeptide works as a motor, because the purified fraction could not drive the movement of actin filaments. One possibility is that the 130 kDa polypeptide was proteolytically inactivated during purification. To minimize this possibility, the cells were homogenized in a solution containing 1% w/v casein to protect the 130 kDa polypeptide from protease, but the purified fraction still failed to drive actin movement. Another possibility is inactivation of the motor activity with high concentration of salt, but the combination of high salt and ATP was the only condition found to effectively release the 130 kDa polypeptide. Thus, improvement of the elution conditions is an essential step to further characterize the protein.

To obtain more insight into the relationship between the 130 kDa polypeptide and gliding motion, I prepared an anti-130 kDa polypeptide antibody and investigated its localization in the cell. The frustule of *Pleurosigma* sp. has many small pores, but the antibodies penetrate poorly into intact cells. Therefore, immunofluorescence microscopy

was performed after fixation and disruption of the cell. The 130 kDa polypeptide localized to the along the actin bundles, as expected from the biochemical experiments, but also was found on both sides of the raphe even in the absence of the actin bundles. Unfortunately, from the technical difficulty of permeabilizing the silicified cell wall of *Pleurosigma*, I could not examine localization of the 130 kDa polypeptide in a whole-cell specimen. However, the localization of the 130 kDa polypeptide observed here is consistent with the hypothesis that the 130 kDa actin-binding protein links the actin bundles to a putative transmembrane protein inserted into the cell membrane lining the raphe to drive gliding.

In summary, all pieces of evidence provided by my work here support the idea that the 130 kDa polypeptide is a myosin-like protein and is involved in the gliding motion in *Pleurosigma* sp. To make sure of the relationship between the 130 kDa polypeptide and gliding motion, the following studies should be carried out: First, *in vitro* motility of actin filaments should be reconstituted with the purified 130 kDa polypeptide. Inhibition of the *in vitro* motility with 130 kDa polypeptide antibody will provide a critical piece of evidence for the involvement of the 130 kDa polypeptide, as an actin-based motor, in gliding motion. Second, precise distribution of the 130 kDa polypeptide in the *Pleurosigma* sp. cell should be examined by immuno-electron microscopy using the anti-130 kDa polypeptide antibody to show that the 130 kDa polypeptide is indeed located in a position consistent with transducing force generated upon the actin bundles near the raphe to the cell exterior through yet-to-be-identified a transmembrane protein(s) on the cell membrane. Third, although it is difficult, involvement of the130 kDa polypeptide in gliding motion of *Pleurosigma* sp. should be tested directly. My collection of monoclonal antibodies against the 130 kDa polypeptide might provide clues to solving these

challenging problems.

3-5 Figures

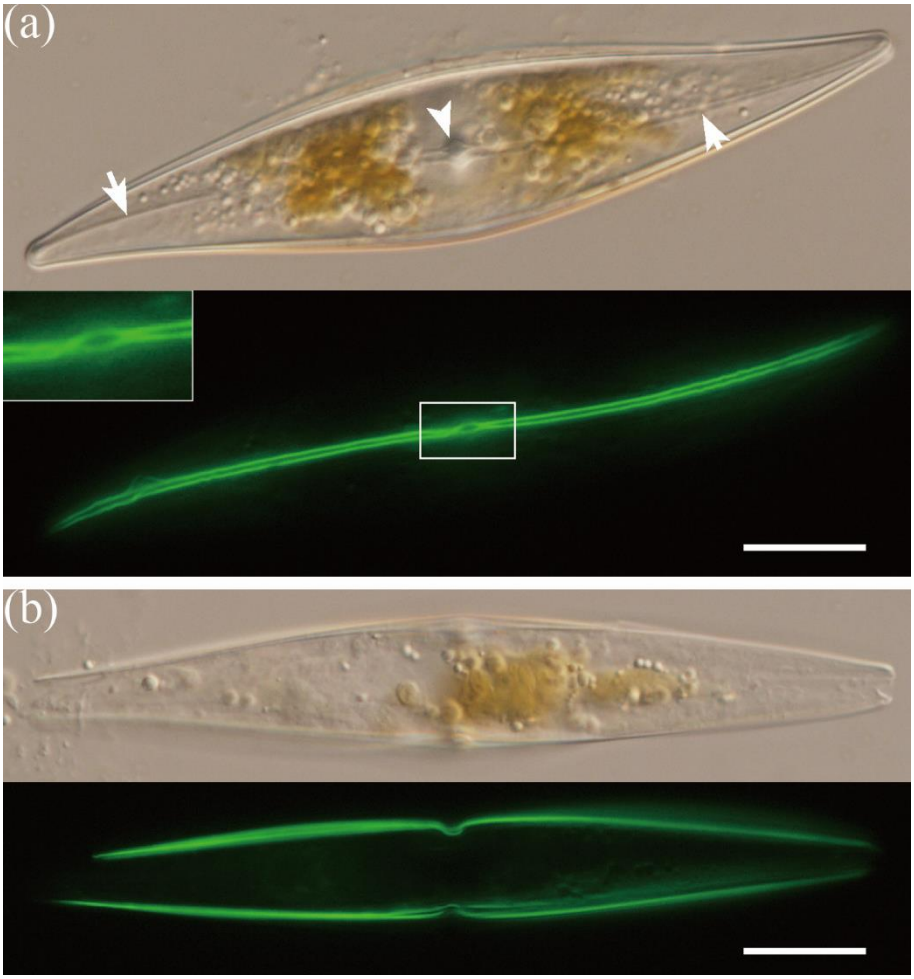

Fig. 3-1. Alexa Fluor 488-labeled phalloidin staining of *Pleurosigma* sp. (a) A top view of a *Pleurosigma* sp. cell stained with Alexa Fluor 488-labeled phalloidin, under the brightfield (upper) or under fluorescence (lower) observations. An arrowhead points to the central nodule. Two arrows point to the raphe. The inset of the upper panel is a magnified view of the boxed region. Prominent S-shaped staining along the raphe is observed. Bar = 20 μm. (b) A side view of a phalloidin-stained cell, observed under brightfield (upper) or under fluorescence (lower) observation. It is to be noted that actin bundles were bend at the middle of the cell. Bar = 20 μm.

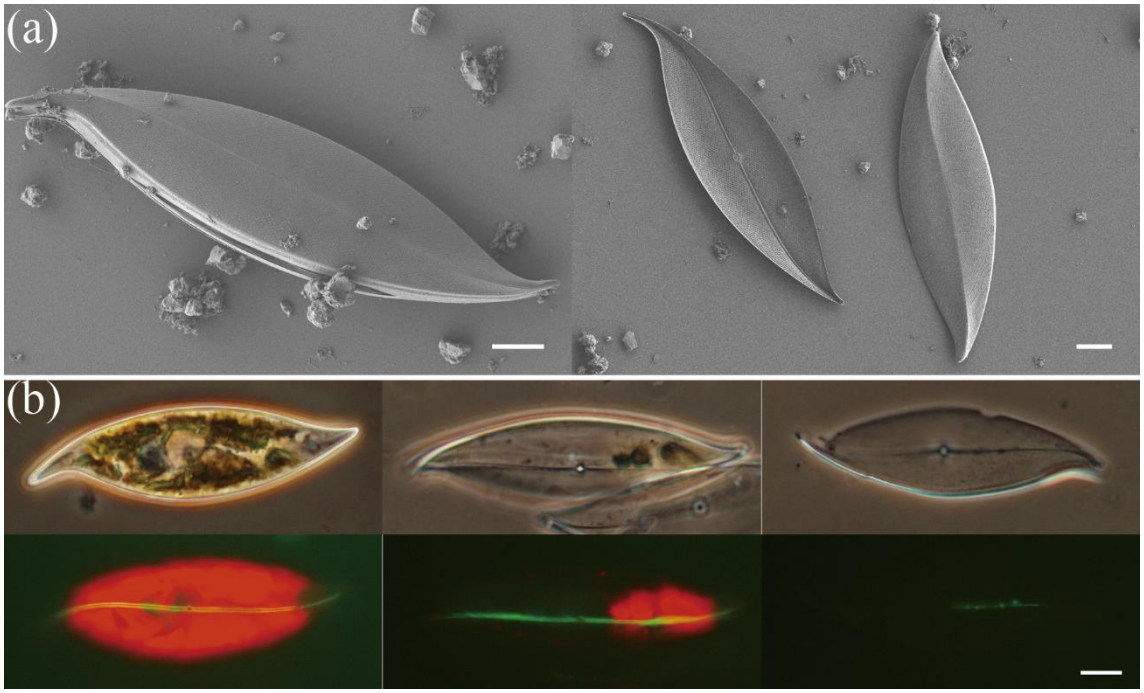

Fig. 3-2. Morphology of *Pleurosigma* sp. cells before and after cell disruption with beads. (a) SEM observations of *Pleurosigma* sp. valves before (left) and after (right) cell disruption by vigorous agitation with glass beads. A set of two valves in the intact cell is fit with each other in the left panel. On the other hand, individual valves release from cells are observed after cell disruption. Bars = 10 μm. (b) Phalloidin staining of samples in (a). A pair of two images represents a phase contrast image (upper) and a fluorescence image from Alex Fluor 488-labeled phalloidin (lower). The left pair shows a cell before disruption with beads. The middle shows a cell after disruption. The right shows the valve extensively washed with buffer after cell disruption. Green fluorescence means the actin staining, and red means the autofluorescence of chloroplasts. Bar = 20 μm.

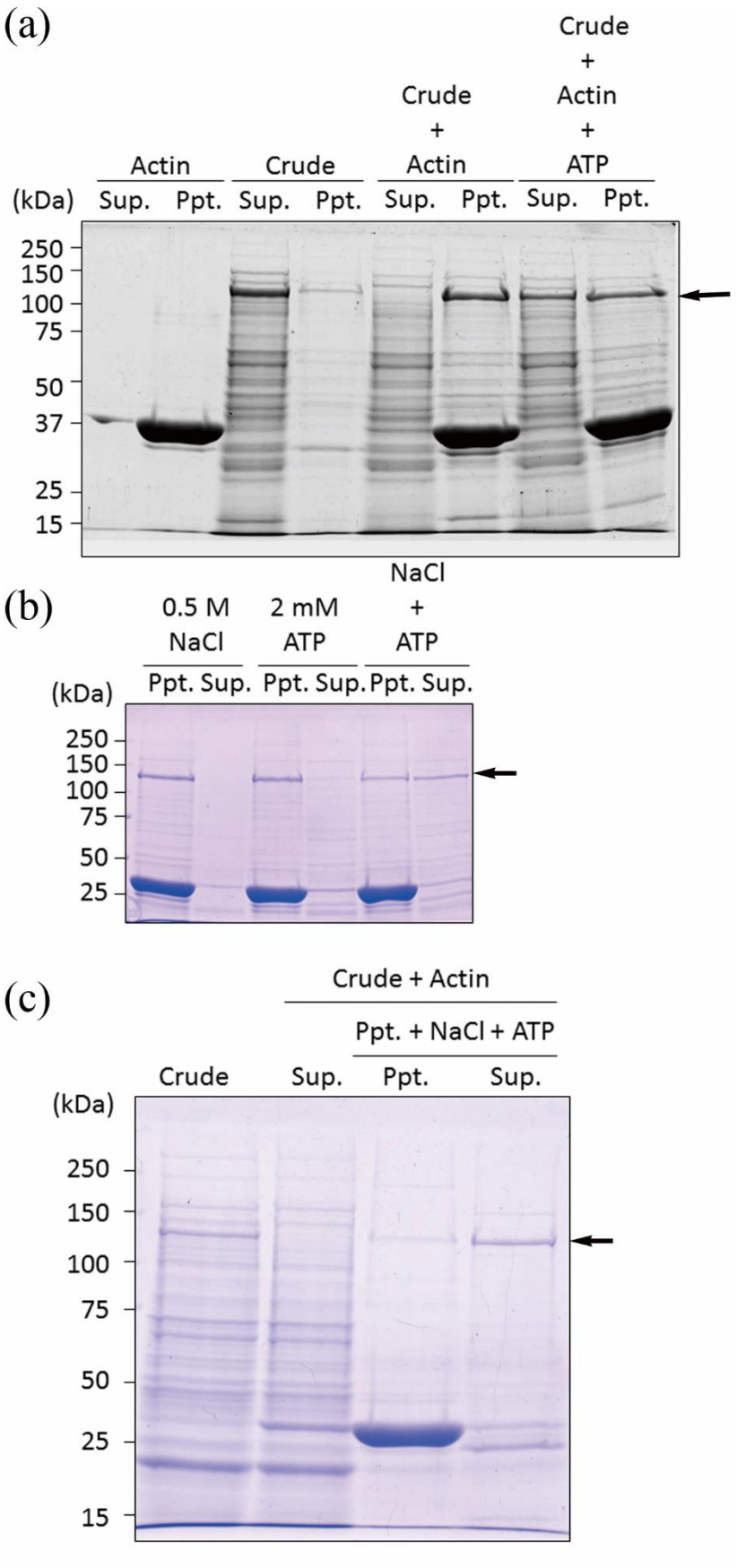
(a)
Actin
Crude
Crude + Actin
Crude + Actin + ATP
(kDa)
Sup. Ppt. Sup. Ppt. Sup. Ppt. Sup. Ppt.
250
150
100
75
50
37
25
15
(b)
0.5 M NaCl
2 mM ATP
NaCl + ATP
(kDa)
Ppt. Sup. Ppt. Sup. Ppt. Sup.
250
150
100
75
50
25
(c)
Crude + Actin
Ppt. + NaCl + ATP
Crude
Sup.
Ppt.
Sup.
(kDa)
250
150
100
75
50
25
15

Fig. 3-3. Preparation of the 130 kDa polypeptide from the extract of the cell hulls of *Pleurosigma* sp. (a) Association of the 130 kDa polypeptide in the cell hull extract of *Pleurosigma* sp. with actin. A salt extract of the cell hulls (crude extract) was subjected to co-precipitation with chicken skeletal muscle actin filaments. Lanes "Actin": chicken skeletal muscle actin alone was separated into a supernatant (Sup.) and a precipitate (Ppt.) by centrifugation. Lanes "Crude": the crude fraction extracted from the cell hulls was subjected to centrifugation. Lanes "Crude + Actin": a mixture of the crude fraction and actin was centrifuged. Lanes "Crude + Actin + ATP": a mixture of the crude fraction and actin supplemented with 2 mM ATP was centrifuged. The same volume of the samples was applied to the SDS-polyacrylamide gel, and protein bands were visualized by CBB staining. (b) Optimization of conditions for the 130 kDa polypeptide elution from the actin co-precipitate. Lanes "0.5 M NaCl": the co-precipitate was incubated with a buffer containing 0.5 M NaCl, and then separated by centrifugation. Lanes "2 mM ATP": the co-precipitate was incubated with a buffer containing 2 mM ATP, and centrifuged. Lanes "NaCl + ATP": the co-precipitate was incubated with a buffer containing both 0.5 M NaCl and 2 mM ATP. (c) Large scale isolation of the 130 kDa polypeptide from the crude fraction. The left most lane: the crude fraction subjected to actin co-precipitation. The second lane: the supernatant of the actin co-precipitation. The third lane: the precipitate of centrifugation after elution with 0.5 M NaCl and 2 mM ATP. The right most lane: the supernatant of centrifugation after the elution.

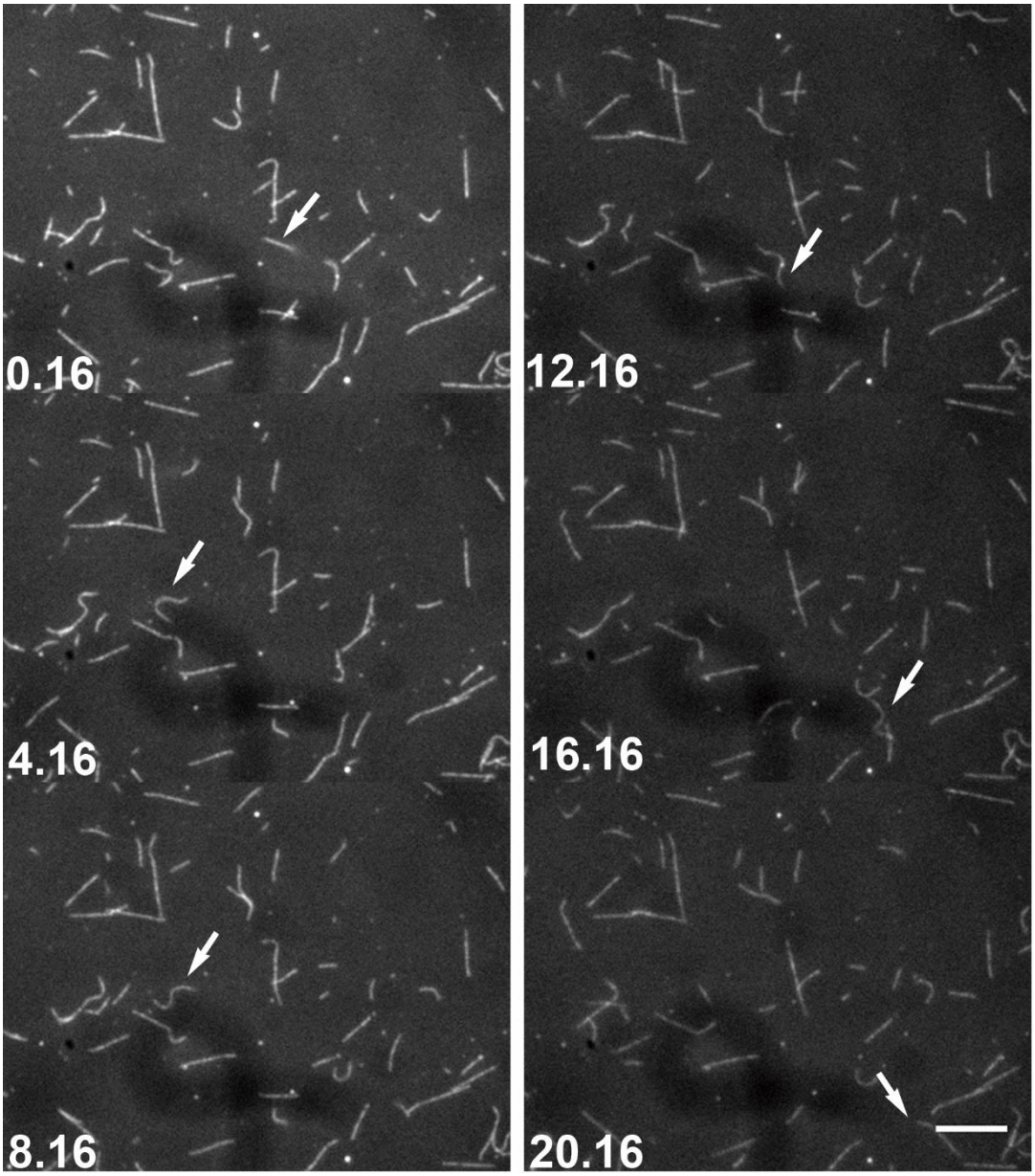

Fig. 3-4. Time-lapse micrographs of the *in vitro* motility assay with the crude fraction. The movement of rhodamine-phalloidin-labeled chicken muscle actin filaments on a glass slide coated with the crude fraction containing the 130 kDa polypeptide was monitored in the presence of 2 mM ATP at room temperature under the fluorescence microscope. Frames of every 4 sec. were shown, and duration after the beginning of recording is indicated on the lower-left corner. Arrows follow a sliding actin filament. Bar = 20 μm.

(a)

```
Pl p130 ------------------------------ELIESRTGLCAMLNEECVRP--
Pt MyoA EDVFRAVQAEYEAEGIALAEIQYDDNTDVLDLIEGRSGLLAMLNEECVRPKG 580
Pt MyoC EDIFRSVQTEYEAEGIELAEIWYDDNTDVLDLIEGRTGLLALLNEECVRPQG 575
Pt MyoE RDIFQTVQEEYKFEGIRLDDIMYDNNTDVLDLIEGRGGLLAILNEECVRPKG 571
Pt MyoG QDIFRSVQAEYETEGIELEEITYDDNTDVLDLVEGRMGLLAVLNEECVRPGG 586
Cg Myo1b LTLKEEQEEYIREDIEWTHIDYFNNAVICELIENNTNGILAMLDEECLRPG 385
```

(b)

	Length	Mass(kDa)	E-val.	Identity(%)	Similar(%)
Pt MyoA	1110	126.4	0.0079	80.0	95.0
Pt MyoC	1157	131.2	0.011	80.0	95.0
Pt MyoE	1159	132.0	0.099	75.0	90.0
Pt MyoG	1257	142.4	0.14	70.0	90.0
Cg Myo1b	1023	118.8	0.4	66.7	85.7

Fig. 3-5. A partial amino acid sequence of the 130 kDa polypeptide. (a) Sequence alignment of the partial amino acid sequence obtained from the 130 kDa polypeptide (Pl p130) against diatom myosins of *P. triconatum* (Pt MyoA, C, E and G) and myosin Ib of *Cricetulus griseus*, Chinese hamster (Cg Myo1b). Identical residues between the 130 kDa polypeptide partial sequence and at least one of the diatom myosins are indicated by yellow background. Conserved substitutions in all the sequences are indicated by gray background. Numbers represent amino acid-residue numbers of the respective proteins. (b) Summary of the sequence comparison.

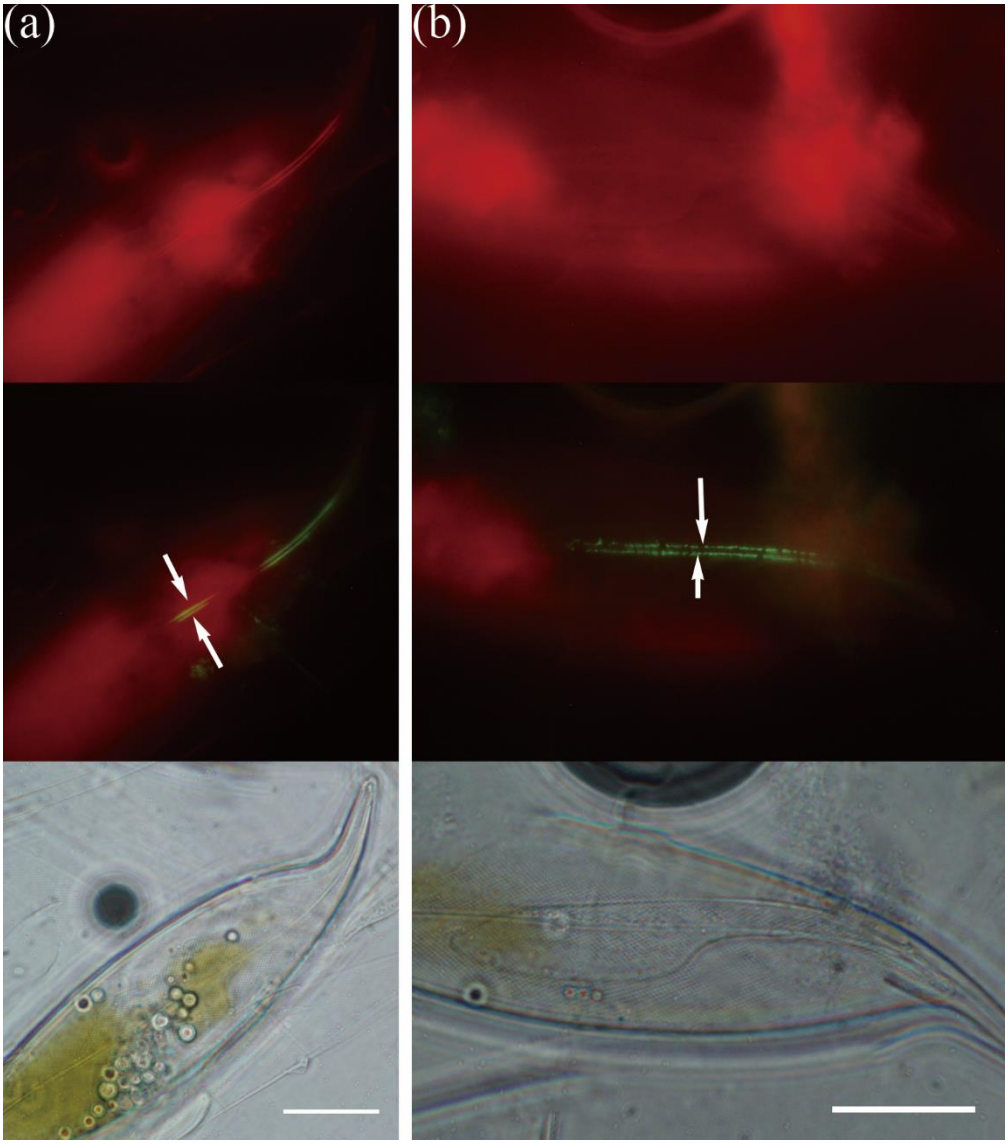

Fig. 3-6. Double staining of actin and the 130 kDa polypeptide in *Pleurosigma* sp. cells. Opened cell hulls prepared as in Fig. 3-2 were subjected to rhodamine-phalloidin and anti-130 kDa polypeptide antibody staining. A set of three images consists of an actin staining with rhodamine-phalloidin (top), anti-130 kDa polypeptide antibody staining (middle), and brightfield (bottom). Large amorphous red fluorescence in the upper two panels corresponds to auto-fluorescence of chloroplasts. Green signals marked by arrows represent the 130 kDa polypeptide. (a) The valve showed partial co-localization of the 130 kDa polypeptide (two green juxtaposing lines in the middle panel) with actin bundles

(thin red strings shown in the top panel). (b) There is no actin bundles detected in the top panel, but the130 kDa polypeptide gave dotty signals along both sides of the raphe in the middle panel. Bar = 20 μm.

Chapter 4

Mucilage movement of gliding diatoms

4-1 Introduction

Some pennate diatoms can adhere to the substratum and glide on it but the molecular mechanism of this motion is not fully understood. It has been postulated that the motion depends on the extracellular mucilage whose movement is driven by intracellular actomyosin (Edgar and Pickett-Heaps, 1984; Wetherbee *et al*., 1998).

In unicellular diatoms, mucilage is thought to be secreted near the raphe by exocytosis and to link the cell body to the substratum accompanied by movement along the raphe (Drum and Hopkins, 1965; Harper and Harper, 1967; Edgar and Pickett-Heaps, 1982; 1983; Webster *et al*., 1985; McConville *et al*., 1999), and its motive force is generated by actomyosin (Poulsen *et al*., 1999; this study). In previous studies, the morphology and localization of mucilage was analyzed by electron microscopic observation (Edgar and Picket-Heaps, 1982; Edgar, 1983), and by light microscopic observation with microbeads or antibody decoration (Picket-Heaps *et al*., 1991; Lind *et al*., 1997). From those results, it has been proposed that the motive force for gliding motion is transmitted to the cell exterior by a putative transmembrane protein(s) that links the motor complex to the mucilage, connecting the cell surface to the substratum. However, I have found no real-time observation of moving mucilage during gliding in the literature. In a colonial diatom, *Bacillaria paxillifer*, it was also reported that mucilage extends from the raphe and presumably links the two adjacent cells (Schmid, 2007). However, again, real-time observations of movement of mucilage are apparently absent from the literature.

To visualize mucilage in gliding diatoms, I stained it with fluorescein-labeled lectins because the mucilage is reported to contain sugar (Lind *et al*., 1997) and succeeded in observing it in *Pleurosigma* sp., and *B. paxillifer*, during gliding.

4-2 Materials and Methods

Cell culture

Both of *B. paxillifer* and *Pleurosigma* sp. were cultured as described in Chapter 2 and 3. For mass culturing of both diatoms, cells were cultured in an artificial seawater, Marine Art SF-1 (ASW; Tomita Pharmaceutical Co., Tokushima, Japan) supplemented with IMK Medium and Na_2SiO_3 at shallow styrol boxes. The culture was kept near the window on the north side at room temperature throughout the year.

Observation of diatoms treated with fluorescein-labeled lectins

Cells were collected by filtration with nylon filter having a passage aperture of 30 μm (Nippon Rikagaku Kikai Co., Tokyo, Japan), rinsed three times for 5 min each in ASW filtrated with a 0.22 μm sterile filter unit equipped with an MF-Millipore MCE membrane, stained with one of the fluorescein-labeled lectins in Table 1 (Fluorescein lectin kit I-III, Vector Laboratories, Inc., Burlingame, CA, USA) at a final concentration of 10 μg/mL in a dark room for 1 to 3 hrs at room temperature. In the case of *B. paxillifer*, the cells were rinsed in filtered ASW once to remove excess fluorescein-labeled lectin after incubation. After lectin decoration, both diatoms were suspended in ASW and placed on an uncoated glass slide at room temperature. Fluorescence was monitored through an epifluorescence microscope (either BX-50 or BX-60; Olympus) fitted with a CCD camera, DP-73 or Victor KY-F550 (JVC Kenwood, Kanagawa, Japan). Frames with a defined time interval were extracted from a digital movie recording of the cell motion, and the distance was measured. Quantitative analysis of cell motion was performed with the NIH ImageJ software as described in Chapter 2.

Trail visualization with micro beads

Pleurosigma sp. cells suspended in ASW were placed on an uncoated glass chamber at room temperature. Microbeads, 0.2% carboxylate-modified microspheres 2.0 μm in diameter (Invitrogen, Carlsbad, CA, USA), in the ASW were perfused into the chamber and rinsed with ASW several times by perfusion to remove the excess beads. Then, beads attached to the trail were observed through bright-field microscopy on an Olympus BX-60 stand fitted with a CCD camera (JVC Kenwood, DP-73).

The effect of lectin on gliding motion of *B. paxillifer*

Concanavalin A (Wako) was dissolved in ASW to make a 40 mg/mL stock solution and was stored at −20°C. The stock solution was diluted in ASW as indicated, and *B. paxillifer* colonies on a glass slide were soaked in this working solution by perfusion. Controls received equivalent volumes of ASW. The gliding colonies were counted in the the bright-field microscope as described above.

Table 1. The abbreviation and affinity list of fluorescein-labeled lectins

Abbreviation	Full name	Sugar specificity
Con A	Concanavalin A	Man α, Glc α
DBA	*Dolichos biflorus* agglutinin	GalNAc α
DSL	*Datura stramonium* lectin	$(GlcNAc)_2$
ECL	*Erythrina cristagalli* lectin	Gal β 1-4 GlcNAc
GSL I	*Griffonia (Bandeiraea) simplicifolia* lectin I	Gal α, GalNAc α
GSL II	*Griffonia (Bandeiraea) simplicifolia* lectin II	GlcNAc α, GlcNAc β
Jacalin	-	Sialyl-Gal β 1-3 GalNAc-O-
LCA	*Lens culinaris* agglutinin	Man α
LEL	*Lycopersicon esculentum* lectin	$(GlcNAc)_n$
PHA-E	*Phaseolus vulgaris* Erythroagglutinin	Oligosaccharide
PHA-L	*Phaseolus vulgaris* Leucoagglutinin	Oligosaccharide
PNA	Peanut agglutinin	Gal β 1-3 GalNAc
PSA	*Pisum sativum* agglutinin	Man α
RCA I	*Ricinus communis* agglutinin I	Gal β
SBA	Soybean agglutinin	GalNAc
STL	*Solanum tuberosum* lectin	$(GlcNAc)_3$
S-WGA	Succinylated-Wheat germ agglutinin	$(GlcNAc)_n$
UEA I	*Ulex europaeus* agglutinin I	Fuc α
VVA	*Vicia villosa* agglutinin	GalNAc
WGA	Wheat germ agglutinin	$(GlcNAc)_n$, Sialic Acid

Gal: D-Galatose, GalNAc: *N*-Acetyl-D-galactosmine, Glc: D-Glucose, GlcNAc: *N*-Acetyl-D-glucosamine, Fuc: L-Fucose, Man: D-Mannose.

4-3 Results

4-3-1 A search for lectins binding to mucilage of the unicellular diatom, *Pleurosigma* sp.

Unicellular diatoms are assumed to secrete mucilage to attach themselves to the substratum and to glide on it. To investigate movement of the mucilage *in vivo*, I sought indicators to specifically detect mucilage in living cells. Because mucilage is supposed to contain polysaccharides, I screened lectins that bind to mucilage by staining the unicellular diatom, *Pleurosigma* sp. with 20 different fluorescein-labeled lectins (Table 1).

While most if not all lectins stained the cell surface (Fig. 4-1), a few appeared to stain gliding mucilage. The clearest candidate for a lectin that stained gliding mucilage was the succinylated-wheat germ agglutinin (S-WGA), which recognizes *N*-acetylglucosamine., In addition to staining the upper and lower surface of the valves as did most lectins, S-WGA stained the raphe in a punctate pattern and an array emanating from the raphe that appeared to follow the path of gliding (Fig. 4-1, S-WGA, arrowheads). Curiously, wheat germ agglutinin (WGA) stained the cell tips (Fig. 4-1, WGA, arrowheads), despite the fact that WGA can bind both *N*-acetylglucosamine and sialic acid.

Concanavalin A (Con A), *Lens culinaris* agglutinin (LCA), and *Pisum sativum* agglutinin (PSA) stained the surface of the cells and sometimes periphery of the raphe (Fig. 4-1, Con A, LCA and PSA). PSA also stained the girdle band as a line (Fig. 4-1, PSA, arrow). Nevertheless, although staining appeared to be localized to specific parts of the frustule, it did not seem to be related to gliding because they did not change their localization during gliding, and were not observed in the gliding trail. The other 15 lectins

screened bound to the whole surface of the cells strongly or weakly, and were sometimes observed near the raphe. But again, their localization did not change during gliding (Fig. 4-1). Thus, hereafter, I used S-WGA to visualize mucilage of *Pleurosigma* sp.

4-3-2 Analysis of mucilage dynamics of *Pleurosigma* sp. with fluorescent- S-WGA

To elucidate relationship between gliding and mucilage, I monitored localization and dynamics of mucilage stained with S-WGA in living *Pleurosigma* sp. cells. When cells gliding in fluorescein-S-WGA containing medium were monitored under the fluorescence microscope whose focus was adjusted to the substratum side of the cell surface, fluorescent puncta or amorphous aggregates with a diameter less than 5 μm, appeared first at the forward end of the raphe intermittently. The S-WGA-positive material seemed to be attached to the substratum insofar as the position of the fluorescence against the substratum usually changed little if at all during gliding of the cells (Fig. 4-2, arrows). From the viewpoint of the diatom cell, fluorescence seemed to move along the middle line of the valve corresponding to the raphe. A punctum sometimes stopped at the center of the valve corresponding to the central nodule, and then resumed movement along the raphe. Eventually, the S-WGA binding material departed from the rearward end of the cell (Fig. 4-2a, arrows). The S-WGA binding material appeared to be secreted from the raphes of both in epi- and hypo-valves (Fig. 4-2b, arrows), but the shape, size and release interval of fluorescent material t appeared to be distinct between the epi- and hypo-valves. The S-WGA binding material appearing on the epi-valve was also secreted from the front end of the cell and remained associated with the cell until it reached the rearward end of the epi-valve. Then, the material was released from the cell and became suspended in the medium.

When I observed S-WGA fluorescence bound to the trail of a gliding diatom, I noticed that the spots appeared as though connected along a thread. Fig. 4-3a shows an example of a trail that consisted of aligned spots stained with S-WGA left behind a gliding cell (Fig. 4-3a, arrows). The trails could be stained by non-specific adhesion of negatively charged microbeads, and most of these trails had short regions where microbeads were absent (Fig. 4-3b, arrows). Furthermore, some gliding cells without a trail stained with labeled S-WGA were sometimes observed. These results suggest that *Pleurosigma* sp. secretes material from both the epi- and hypo-raphes during its gliding, and the S-WGA-positive compound is often but not always present.

4-3-3 A search for lectins binding to mucilage of the colonial diatom, *Bacillaria paxillifer*

It was reported that mucilage plays an important role in conjugation of adjacent cells in a colony of *B. paxillifer,* and mucilage between adjacent cells should be stable and not easily dislodged to keep adjacent cells associated with each other, even when the colony becomes extended (Schmid, 2007). Thus, properties of mucilage in *B. paxillifer* seem to be different from those of unicellular diatoms. To visualize mucilage in *B*. *paxillifer*, I again examined the set of 20 fluorescein-labeled lectins, and in this case found that Con A stained the spaces between adjacent cells of *B. paxillifer* strongly (Fig. 4-4, Con A and Fig. 4-5a, arrows). In addition, the pattern of Con-A fluorescence changed during gliding of individual cells in a colony, suggesting that materials decorated with Con A have some relation to intra-colonial gliding.

The *Ricinus communis* agglutinin I (RCA I) was strongly localized to the space between dividing cells (Fig. 4-4, RCA I, arrow). In contrast, LCA was localized near both

sides of the nucleus as well as to the space between the dividing cells (Fig. 4-4, LCA, arrows). WGA was strongly localized to the surface of the whole colony (Fig. 4-4, WGA). These staining patterns seemed to be specific, but relationship to the gliding motion was obscure because these patterns did not change appreciably during gliding motion. The other 16 lectins often bound weakly to the entire surface of the *B. paxillifer* colony, probably through non-specific interaction, in patterns that remained constant during gliding.

4-3-4 Motion analysis of the material stained with Con A in *B. paxillifer*

I investigated the localization and morphology of Con A binding material further to clarify the relationship between gliding and the lectin binding material (Fig. 4-5). Fig. 4-5b shows quantitative analysis of the Con A fluorescence during gliding. The intensity and width of the fluorescent areas, in addition to the distance between the tips of a pair of two adjacent cells in a *B. paxillifer* colony were measured as a function of time. Average intensity of a fluorescent area between adjacent cells was lowest when the colony narrowed and highest when the colony was fully extended. Con A seemed to be associated with the intracellular interface stably because integrated intensity of the fluorescent areas remained constant for more than 1 hr, even after washing out unbound labeled Con A. The width of the fluorescent areas became maximum when the distance between the tips of the adjacent cells was minimum, and became minimum when the colony was fully extended. These results indicate that the Con A binding-material is elastic and maintained between the adjacent cells during gliding of the colony. It is possible that this material plays an important role in the transduction of the motion force generated by the actomyosin system in the diatom cells.

4-3-5 Effects of lectins on diatom gliding

Because the movement of the Con A binding-material reported above was correlated with intra-colonial gliding of *B. paxillifer*, I predicted that a high concentration of Con A would affect the gliding motion. To investigate the effects of the lectin on the gliding motion, I treated the colonies with various concentrations of Con A. Fig. 4-6 shows that the population of gliding colonies decreased as a function of increasing concentration of Con A. This suggests that some Con-A binding material, which is expected to have α-mannoside residues on its surface, has a crucial role in the gliding motion. However, more than 10 mg/mL Con A was required for complete inhibition of *B. paxillifer* gliding. Thus, I could not rule out a possibility that this inhibition by Con A comes from non-specific coating of the cell surface of the diatom with any protein.

4-4 Discussion

Mucilage secreted from the raphe of diatoms is thought to be composed of polysaccharides and glycoproteins but the chemical components have been scarcely characterized (Picket-Heaps *et al*., 1991; Lind *et al*., 1997). I demonstrate here that the components of extracellular materials of two kinds of diatoms, unicellular *Pleurosigma* sp. and colonial *B. paxillifer*, indeed contain saccharide residues but are different through lectin-staining experiments. The extracellular material of *Pleurosigma* sp. was stained with succinylated-WGA (S-WGA), which recognizes poly-*N*-acetyl-D-glucosamine, while the material was not stained with WGA, which recognizes both poly-*N*-acetyl-D-glucosamine and sialic acid. These lectins might distinguish small differences in branching structure, for example, of poly-*N*-acetyl-D-glucosamine. In contrast, the extracellular material of *B. paxillifer* was stained with Con A, which recognizes both α-D-mannoside and α-D-glucoside. LCA also recognizes α-D-mannoside, but the extracellular material of *B. paxillifer* did not react with LCA, suggesting that an α-D-glucoside-containing chemical entity is a component of extracellular material of *B. paxillifer*.

Fluorescence microscopy of the S-WGA-binding material in the living unicellular diatom, *Pleurosigma* sp. revealed that the S-WGA-binding material was secreted at the forward end of the cell, drifted backward along the raphe and finally separated from the cell. Fluorescent puncta often appeared to be trapped temporarily at the center of the cell, probably at the central nodule, then went across it, and finally moved along the rearward raphe. Although secretion of mucilage along both forward and rearward raphes was reported in other unicellular diatoms (Edgar, 1983; Edgar and Pickett-Heaps, 1983), I did not observe any fluorescent spots appearing from parts of the

raphe than its forward end in *Pleurosigma* sp. Because the raphe is interrupted by the central nodule, the part of mucilage containing newly produced S-WGA-binding material should be separated from the cell during passage across the central nodule, and once across should be re-captured by material secreted from the rearward raphe, resulting in a more or less continuous appearance of S-WGA positive mucilage.

During observation, I noticed that *Pleurosigma* sp. cells secrete the S-WGA-binding material intermittently. Indeed, the S-WGA-positive spots in the trail after gliding seemed to be linked by some invisible threads. These results together with the fact that I always observed continuous trails of *Pleurosigma* sp. cells by using polystyrene microbeads (Fig. 4-3b, arrows) and previous reports (Drum and Hopkins, 1965; Harper and Harper, 1967; Edgar and Pickett-Heaps, 1982; 1983; Webster *et al*., 1985; McConville *et al*., 1999) show continuous secretion of mucilage. Unfortunately, I could not find any lectin that stained mucilage or trails continuously among the 20 lectins I examined, suggesting that mucilage is contains unusual polysaccharides. To elucidate dynamics of mucilage and its function in gliding motion of pennate diatoms, it is essential to obtain other types of markers, such as antibodies, that specifically and continuously recognize mucilage.

Does the S-WGA binding material of *Pleurosigma* sp. have any role in gliding motion?. Because the S-WGA-positive spots secreted from the lower raphe during gliding motion seem to be immobilized on the substratum, the material might have a role as a scaffold on the substratum. However, such saccharides should be found always in any mucilage secreted from gliding diatom cells. In my experiments, some *Pleurosigma* cells did not secrete detectable S-WGA binding material but nevertheless glided. Thus, the S-WGA binding material does not seem to have an essential role in gliding. I suppose that

the production of S-WGA-positive mucilage might depend on conditions; for example, temperature, medium composition, and surface properties of the substratum, such as hydrophobicity and electric charges. As conditions vary, likewise the usefulness of the S-WGA positive material for gliding might vary, from essential or irrelevant. Thus, further analyses are required to elucidate involvement the S-WGA binding material in gliding motion of *Pleurosigma* sp.

In a colonial diatom, *B. paxillifer,* the spaces between adjacent cells were stained with fluorescein-labeled Con A. A previous report indicated that adjacent cells were connected through mucilage secreted from the raphe (Schmid, 2007). It is reasonable to assume that Con A binds to such mucilage. Interestingly, the appearance of the fluorescent staining changed concomitantly with the gliding motion; shrinking and brightening during elongation of the colony, and expanding and darkening during its shortening. These changes were documented quantitatively (Fig. 4-5).

Are these changes in Con A binding material driven by the actomyosin system and hence part of the gliding mechanism? So far, I do not have any experimental evidence to answer this question. One apparent experiment to be carried out first is to examine effect of actomyosin inhibitors on movement of the Con A binding material. Particularly, observing the Con A binding material on the free raphe is suitable to evaluate the effect of actomyosin inhibitors. If movement of the Con A binding material is compromised by the inhibitors, then the Con A binding material might have some relation to gliding motion, and Con A could then become a useful tool to investigate contribution of the extracellular material to gliding.

These experiments also indicate that the Con A binding material of *B. paxillifer*

are present stably in mucilage with little if any turnover, which is different from unicellular diatoms, where mucilage is released from the cells during their gliding. The difference of behavior of the lectin binding material in the different diatoms seems to depend on their habitat and metabolism. Unicellular gliding diatoms are benthic, and the sphere of their activity is limited by their gliding, suggesting that they have to move on wide variety of surfaces to find appropriate positions to do photosynthesis. Thus, they acquired an ability to move rather long distances at the cost of discarding mucilage. On the other hand, *B. paxillifer* is a planktonic diatom, living in moving water (ocean or river), suggesting that its locomotion is less important for photosynthesis than that of the benthic diatoms. Therefore, *B. paxillifer* is likely to produce only a limited amount of mucilage.

It is to be noted that the fluorescence intensity of the Con A-positive staining shows almost inverse relation to its width, suggesting that the Con A binding material is associated with some elastic and continuous structure. I found that, when multiple polystyrene beads were attached to a free raphe on a *B. paxillifer* cell, they moved bi-directionally and synchronously. These beads moved almost identically, like beads attached to a single, elastic platform. Therefore, it is possible that such adhesive structures, which might form the connection between adjacent cells, are composed in part of Con A binding material.

I observed inhibition of gliding of *B. paxillifer* by adding a high concentration of Con A. As mentioned in the Results section, I cannot rule out the possibility that this effect is non-specific inhibition of abnormal concentration (>10 mg/mL) of Con A. Thus, further experiments are required to conclude the direct involvement of the Con A binding material in gliding motion of *B. paxillifer*. However, still Con A provides a useful tool to analyze this unique intra-colonial gliding of the diatom.

4-5 Figures

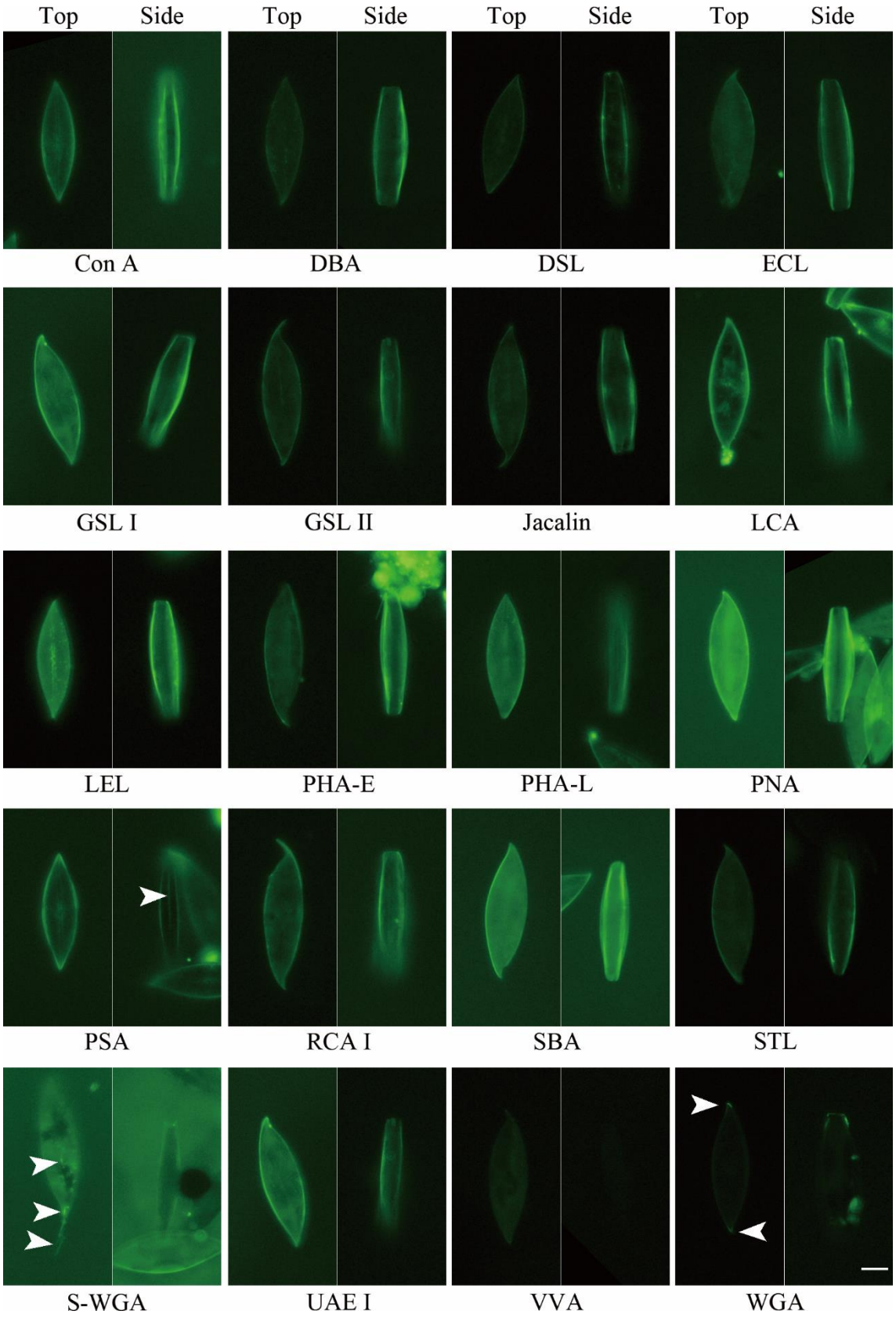
Top
Side
Top
Side
Top
Side
Top
Side
Con A
DBA
DSL
ECL
GSL I
GSL II
Jacalin
LCA
LEL
PHA-E
PHA-L
PNA
PSA
RCA I
SBA
STL
S-WGA
UAE I
VVA
WGA

Fig. 4-1. Fluorescein-labeled lectins staining of *Pleurosigma* sp. A pair of two images show top (left) and side (right) views under the fluorescence microscope in the presence of fluorescein-labeled lectin indicated. The prominent staining of Con A, LCA and PSA was observed at the edges of a cell. WGA stained the both end of the valve, and S-WGA stained the materials came from the raphe and in the trail. Other lectins stained whole cells weakly. Arrowheads show the prominent staining on the cell. Bar = 20 μm.

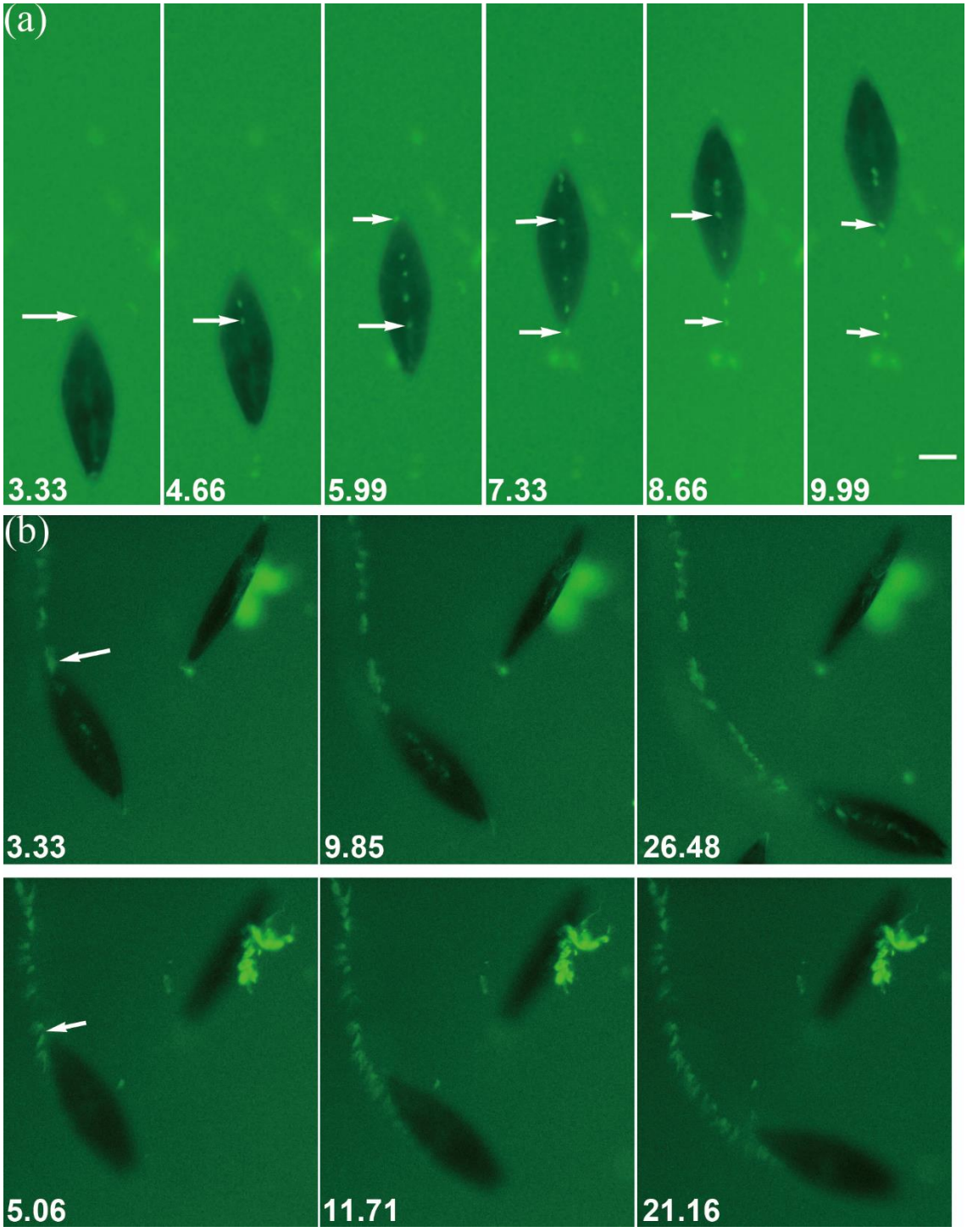

Fig. 4-2. Time-lapse observations of fluorescein-labeled S-WGA staining of *Pleurosigma* sp. (a) The movement of materials secreted from *Pleurosigma* sp. and stained with fluorescein-labeled S-WGA is shown in a series of time-lapse micrographs. Focus was adjusted to the substratum side of the cell. The cell and materials were recorded

at the video rate, and time-lapse images at intervals of 1.33 s were shown. Duration after the beginning of recording is indicated on the lower-left corner in second. Arrows point fluorescent spots immobilized on the substratum. Bar = 20 μm. (b) The trail stained with S-WGA is shown in a series of time-lapse micrographs in different focal planes regarding to one cell. The upper row shows images focusing on the epivalve, while the lower row shows those focusing on the substratum. Duration after the beginning of recording is indicated on the lower-left corner. Bar = 20 μm.

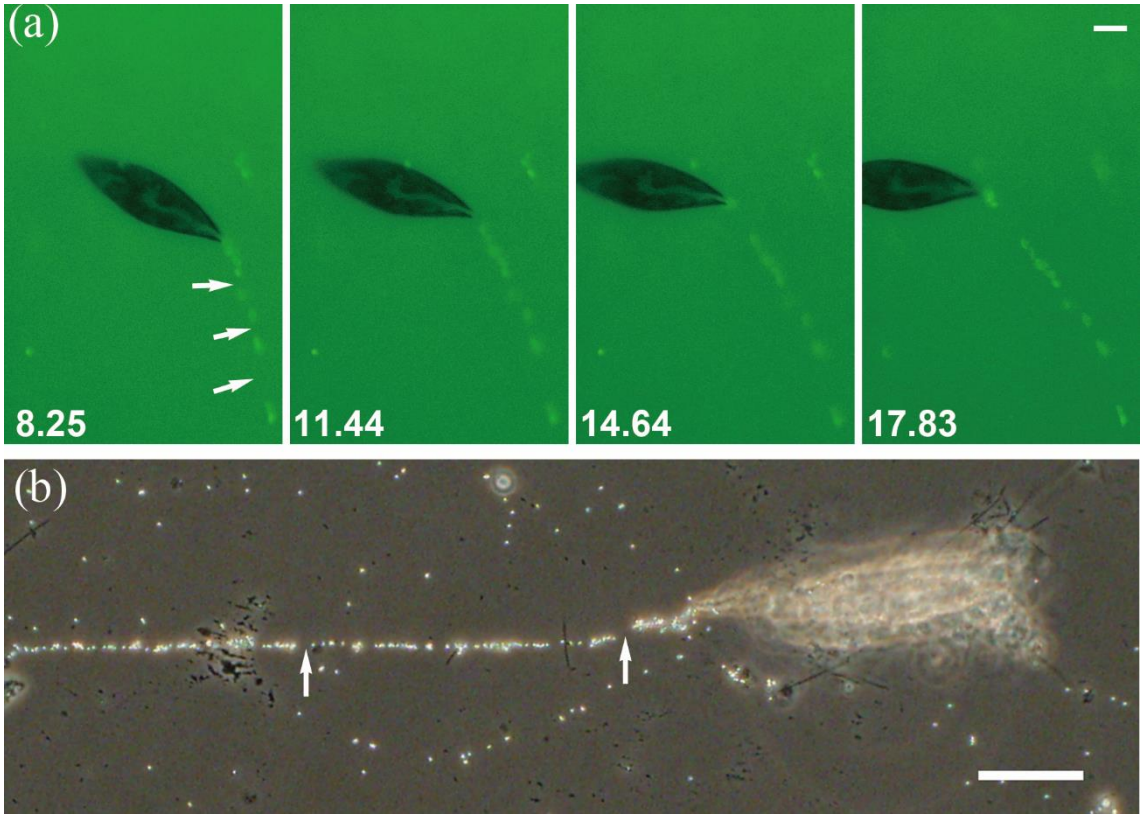

Fig. 4-3. Observations of the trail secreted by *Pleurosigma* sp. (a) A trail formed during gliding of a *Pleurosigma* sp. cell in the presence of fluorescein-labeled S-WGA is shown in a series of time-lapse micrographs. A movie was recorded at the video rate, and time-lapse images at intervals of 3.2 s are shown. Duration after the beginning of recording is indicated on the lower-left corner in second. Arrows indicate regions without fluorescence signals of a trail produced after diatom gliding. Bar = 20 μm. (b) The trail of *Pleurosigma* sp. was labeled with microbeads, and was observed under the bright microscope. Arrows indicate small gaps of beads attachment sites on mucilage secreted from a gliding diatom. Bar = 20 μm.

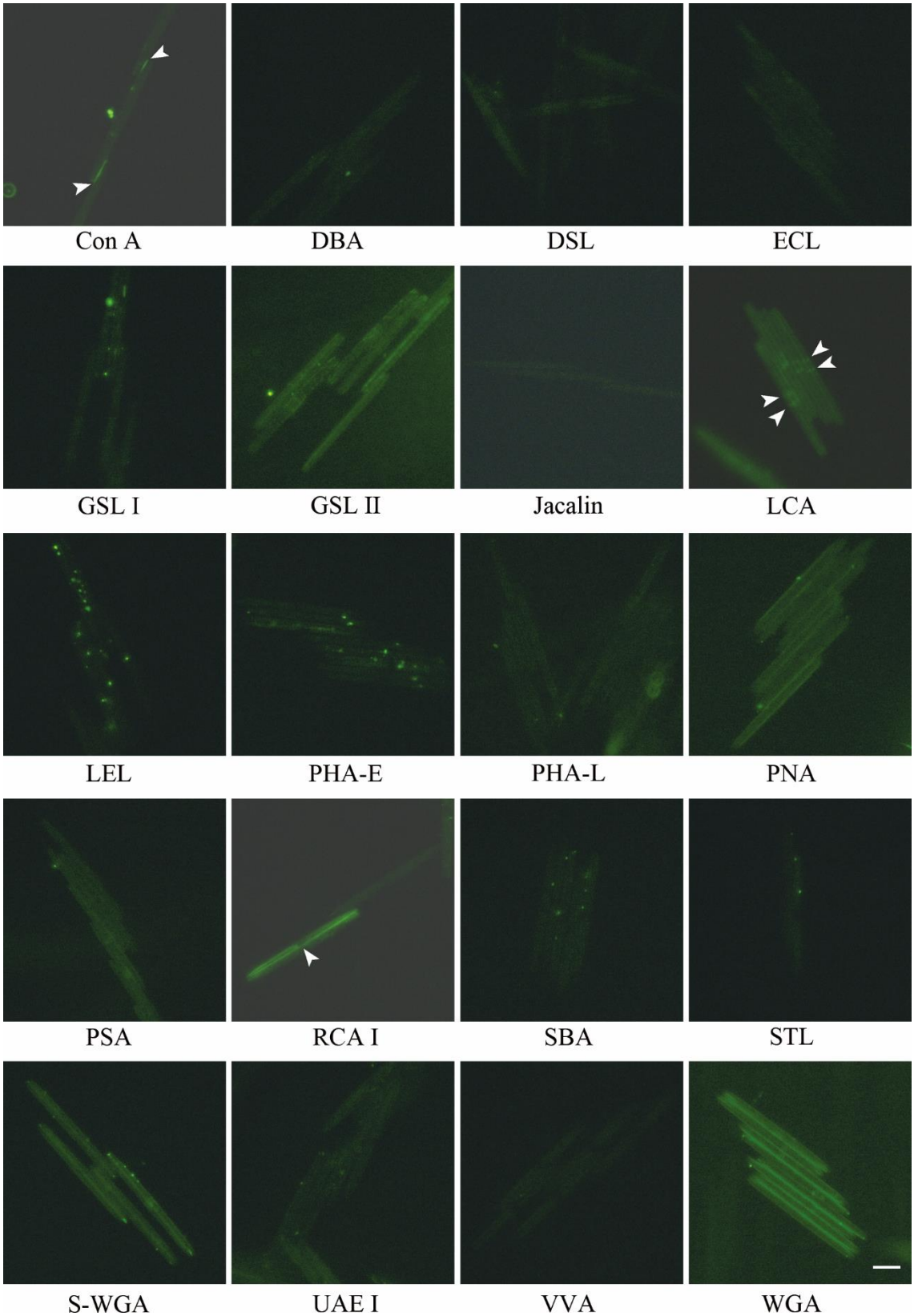

Fig. 4-4. Fluorescein-labeled lectins staining of *B. paxillifer*. A side view of a *B.*

paxillifer colony stained with a fluorescein-labeled lectin indicated under the images. The prominent staining of Con A was observed at the spaces between adjacent cells in a colony, LCA was observed at the space between divided cells and both ends of nuclear, RCA I was observed at the space between divided cells and WGA was observed at the whole of colony. Other lectins stained the diatom colonies weakly and non-specifically. Arrowheads show the prominent staining on the colony. Bar = 20 μm.

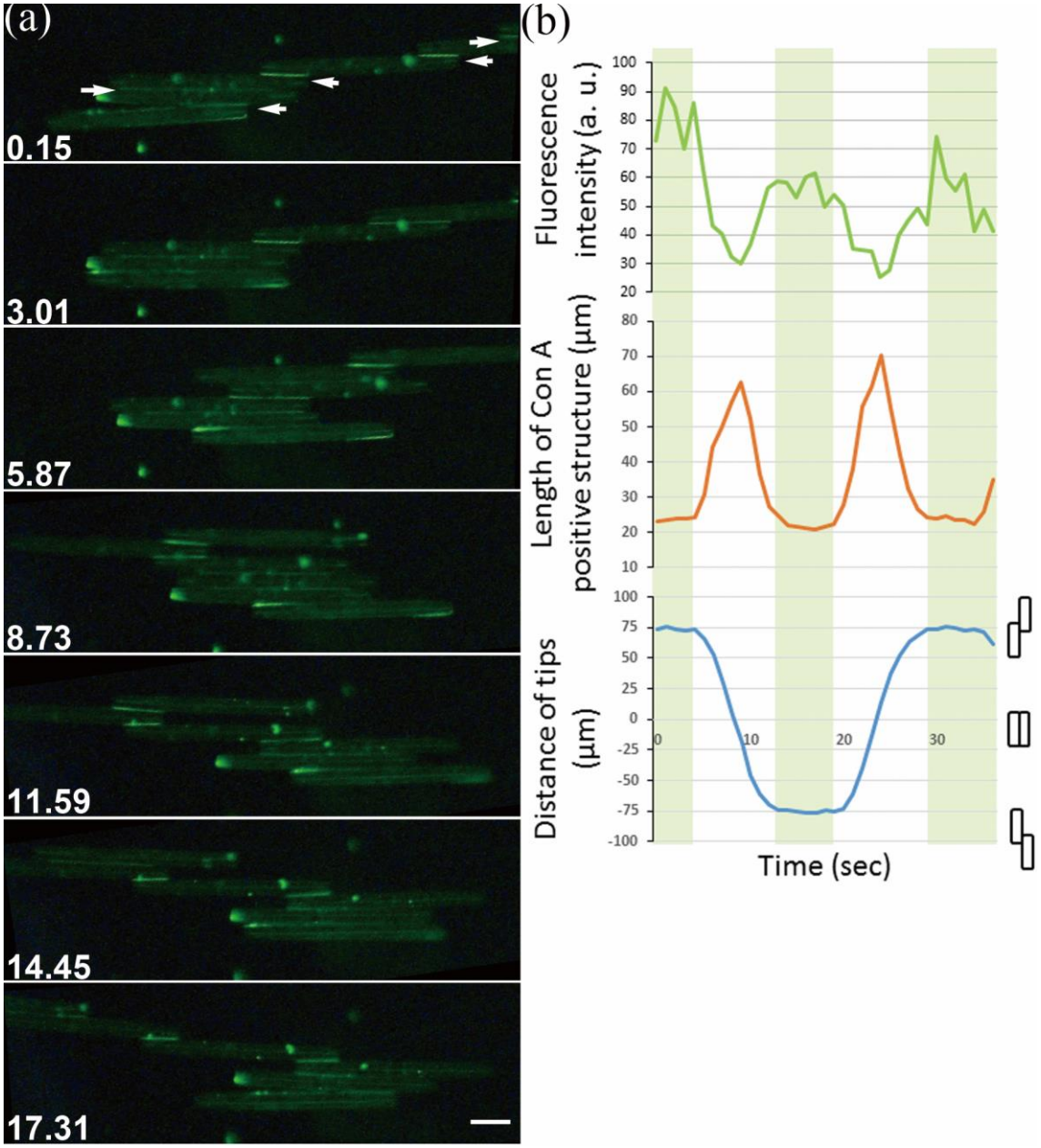

Fig. 4-5. Quantitative analysis of movement of Con A-positive structures and gliding motion of *B. paxillifer*. (a) Typical movement of the Con A-positive structures is shown in a series of time-lapse micrographs. The movie was recorded at the video rate, and time-lapse images at intervals of 2.86 s were shown. Duration after the beginning of recording is indicated on the lower-left corner. Bar = 10 μm. (b) The quantitative analysis of average fluorescence intensity of the Con A-positive region (top), length of the Con A-positive

region (middle), and distance between the tips of two adjacent cells in a *B. paxillifer* colony (bottom). The ordinate, average fluorescence intensity of the Con A-positive region (top), distance of staining mucilage in middle graph (in μm), and distance between tips of the two adjacent cells measured as the length parallel to the longitudinal axis of the cells (in μm); the abscissas, time (in seconds). The schematic drawing of the position of the two adjacent cells is shown in the right.

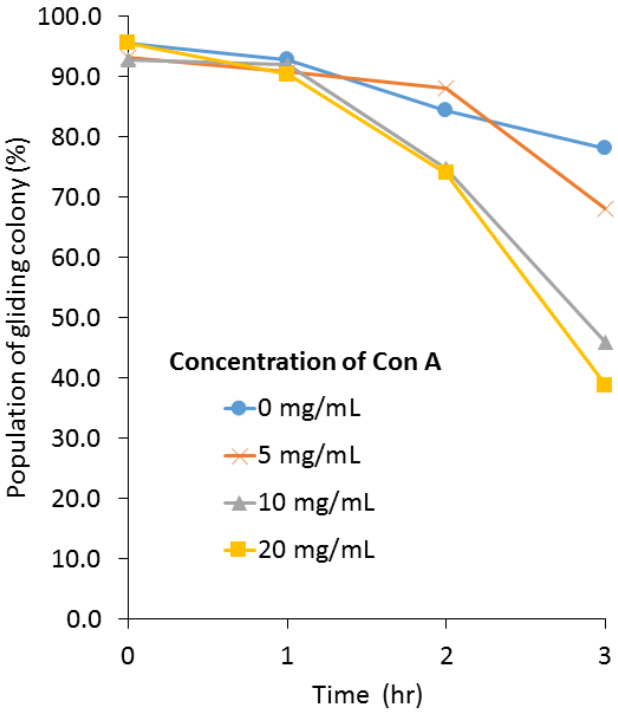

Fig. 4-6. The effect of Con A on gliding motion in *B. paxillifer*. The population of gliding *B. paxillifer* colonies in the presence of indicated concentrations of Con A is shown. The ordinate, percentage of gliding colonies (%); the abscissa, time (in hour). The populations of the gliding colonies in the absence of, 5, 10 and 20 mg/ml Con A is shown in circle (blue line), in cross (red line), in triangle (gray line), and in square (yellow line), respectively.

Chapter 5

General Discussion

5-1 General discussion

In this thesis, I reported involvement of the actomyosin system in the gliding motion of colonial diatom, *Bacillaria paxillifer*. I found actin-like filaments and novel electron-dense structures located between the actin-like filaments and the plasma membrane by electron microscopic observation (Chapter 2). In the unicellular diatom, *Pleurosigma* sp., I isolated a 130 kDa polypeptide as a candidate for a motor protein involved in the gliding motion, and demonstrated that the polypeptide has myosin-like features (Chapter 3). In addition, the fluorescein-labeled lectin staining of both kinds of diatoms, *Pleurosigma* sp. and *B. paxillifer*, enabled me to observe extracellular material *in vivo* and showed that components of the extracellular materials, or mucilage, and their behavior, differ between the two diatoms (Chapter 4).

Previous studies implicated the actomyosin system in gliding motion of the unicellular diatoms, *Navicula cuspidate* and *Craspedostauros australis*, while the precise molecular mechanism of gliding has not been elucidated (Edgar and Pickett-Heaps, 1983; Edgar and Zavortink, 1983; Poulsen *et al*., 1999). In this work, I started with morphological analyses of *B. paxillifer* and *Pleurosigma* sp., and found that these two different types of diatoms have two actin bundles along the raphe like the above unicellular diatoms previously investigated. In addition, I demonstrated that both actin

and myosin inhibitors inhibit gliding motion of both kinds of diatoms, indicating that gliding power of these diatoms is generated by the actomyosin system. However, their gliding modes are distinct, especially regulation of directionality in gliding motion and behavior of extracellular material. What causes these differences?

Bi-directional gliding motion was observed in these two types of diatom, but reversal frequency of the gliding direction is different. *Pleurosigma* sp. can glide in one direction for a while, and sometimes glides for distance of several times longer than its cell length. To enable the unicellular diatoms including *Pleurosigma* sp., to glide for a long distance, motor proteins reaching the rearward end of the actin bundles need be recycled to the front end of the cell or new motor proteins recruited there. A possible recycling system is that motor proteins reaching the terminus of one bundle of actin filaments switch to other bundle, which would have the opposite polarity, and thus move in the opposite direction to the front end of the cell. In this case, two actin bundles on each valve should have opposite polarities or both the bundles should consist of actin filaments with mixed polarities. To investigate polarity of the actin bundles, after disrupting cells, remained actin fibers can be decorated with the S1 fragment of myosin and the resulting “arrowhead” structures assayed with electron microscope. If both of the actin bundles along the raphe have the same polarity, then the motor proteins cannot go

back to the front end of the cell just by switching the track they use. Thus, some mechanism other than actin-based movement of the myosin motor, such as diffusion, cytoplasmic streaming, or conveyance by other motors would be required.

On the other hand, in the gliding of *B. paxillifer*, the direction of adjacent cells usually reverses when the cells are fully extended, meaning more frequent reversal than in unicellular diatoms. The motion analysis of *B. paxillifer* cells in a colony also demonstrated that the bi-directional gliding motion has a reasonably well defined periodicity and that neighboring cell pairs appear to have a mechanism to communicate reversal timing with each other. Compared to the unicellular diatom, *B. paxillifer* has unique electron-dense structures, which are assumed to include motor protein(s) and transmembrane protein(s) to transduce moving force from interior to exterior of the cell. If the two actin bundles along the raphe have opposite polarities, and indeed the electron dense structure contains the motor protein, then the motor protein may easily switch from one actin bundle to the other that has the opposite polarity, because the two actin bundles are closely aligned and the electron-dense structures exist in the vicinity of the two actin bundles. If the two actin bundles have the same polarity, then the electron-dense structures should contain a bi-directional motor protein or two kinds of unidirectional motor proteins with opposite moving directions. Again, determination of polarity of the actin bundles in

B. paxillifer is an essential next step.

In addition to the polarity of actin bundles, the properties of motor proteins powering the gliding is also a critical determinant for the mechanism of gliding motion. So far, I isolated a 130 kDa actin-binding polypeptide from *Pleurosigma* sp. Although it has characteristics common to those of myosin, it is still essential to determine whether the 130 kDa polypeptide is indeed a myosin homologue by obtaining its full length cDNA and its nucleotide sequence. It is also necessary to analyze the sliding direction of this protein on actin filaments using an *in vitro* motility assay with polarity marked actin filaments. Isolation of a motor protein(s) from *B. paxillifer* is another experiment to be carried out. If we obtain these data on the motor and above information on the actin bundles, we will learn how the different gliding modes can be achieved in the unicellular and colonial diatoms.

Behavior of the extracellular material, namely mucilage, stained with fluorescein-labeled lectins, differed between the two kinds of diatom. Unicellular diatoms, including *Pleurosigma* sp. studied in this thesis, discard the lectin binding materials continually. On the other hand, a colonial diatom, *B. paxillifer,* retains its lectin binding material located between two adjacent cells during gliding. Therefore, the two types of diatoms seem to have distinct requirements for mucilage production. It was reported that

vesicles apparently containing mucilage are abundant near the actin bundles in a unicellular diatom, *Navicula cuspidata* (Edgar and Pickett-Heaps, 1983), suggesting that the unicellular diatom is ready to produce and to secrete a plentitude of mucilage for gliding. Similarly abundant vesicles appeared absent in the cytoplasm of the *B. paxillifer* cells, suggesting that *B. paxillifer* does not make large amounts of mucilage continually. I suppose that an appropriate amount of mucilage is synthesized during cell division in *B. paxillifer*, because the two adjacent daughter cells remain associated with each other after cell division. To test this hypothesis, it would be useful to measure amounts of mucilage produced by these two types of diatom. Electron microscopy using probes specifically recognizing a component(s) of mucilage will tell whether those vesicles found near the actin bundles in unicellular diatoms are indeed the source of extracellular mucilage.

Edgar (1979) reported that, in several kinds of unicellular diatoms, beads attached to their upper raphe moved opposite to the gliding direction, indicating that the lower mucilage connected to the substratum moved through the raphe to the same direction as the beads attached to the upper mucilage. In this thesis, staining of extracellular material with fluorescein-labeled S-WGA in *Pleurosigma* sp. showed that fluorescent spots appear at the front end of both epi- and hypo-valves, and move rearward (Fig. 4-2b), indicating that movement of the S-WGA binding material in the upper and

lower raphes in *Pleurosigma* sp. is consistent with that of beads in the unicellular diatoms observed in Edgar (1979). On the other hand, the material stained with Con A attached to the top and bottom of a cell in a *B. paxillifer* colony moved in opposite directions (Fig. 4-5a). Thus, motility of the extracellular material in the two kinds of diatom is again seen to differ, although the movement of extracellular material on both upper and lower surfaces is likely to be regulated cooperatively in both of the diatoms. I postulate three possible regulatory elements: the polarity of upper and lower actin bundles, directionality of motor proteins associated with each actin bundles, and the signaling pathway to link the two sides of a diatom cell.

There are several explanations for difference in the gliding modes of the two diatoms. One possibility is that the two actin tracks have opposite polarities on epi- and hypo-valves, suggesting a putative unidirectional motor complex is associated with actin bundles which have the same or opposite polarities between the two valves in *Pleurosigma* sp. or *B. paxillifer*. In this case, the direction of mucilage movement would be caused by the polarity of actin bundle. Another possibility is that the two actin tracks have a single polarity and distribution in both epi- and hypo-valves, requiring unidirectional motors associated with actin bundles in *Pleurosigma* sp. and two kinds of unidirectional motors associated with actin bundles in *B. paxillifer*. In addition, two actin

tracks with a single polarity and opposite distributions on epi- and hypo-valves, two kinds of motors associated with the actin bundles in *Pleurosigma* sp. and one motor associated with the actin bundles in *B. paxillifer*. Thus, the moving direction of mucilage is determined by the feature of motor complexes. To make clear this hypothesis, determination of polarity of actin bundles on each valve and identification of the motor protein from each diatom are required.

Regarding to the signaling pathway, Cooksey and Cooksey (1980) reported that calcium is necessary for gliding motion in the unicellular diatom, *Amphora coffeaeformis*. The movement was inhibited by calcium blocking agents, such as ruthenium red and α-isopropyl-α-[(*N*-methyl-*N*-homoveratryl)-α-aminopropyl]-3,4,5 -trimethoxy phenyl acetonitrile. Significance of free calcium in regulation of cell motility has been generally accepted in many biological systems. If gliding motion was regulated by a calcium-related signaling pathway, visualization of the distribution of calcium in the diatom cells by using a calcium indicator should help understanding the regulatory circuit of the motor complexes associated with the raphes on the opposite sides.

In summary, I provide experimental data to support the idea that gliding motion

of diatoms is enabled by cooperative action of the actomyosin system, structures that link the motor proteins to the extracellular mucilage, and saccharide-containing mucilage adhesive to the substratum. I also show that even among gliding diatoms, unicellular species and colonial species have some essential differences in gliding characteristics. However, a complete understanding of the molecular mechanism of gliding motion of the diatoms remains a distant goal.

Thus, the following studies would be worthwhile to carry out to deepen our understanding. First, the polarity of actin bundles along the raphe should be determined to constrain mechanisms for bi-directional gliding and movement of extracellular material. "Arrowhead formation" with the S1 myosin fragment on the actin filaments and its observations with SEM or TEM should help to define the polarity. Second, involvement of the 130 kDa polypeptide purified from *Pleurosigma* sp. in the gliding motion should be confirmed and characterized further. The *in vitro* motility assay with the purified 130 kDa polypeptide help do this, as will immuno-electron microscopy with the anti-130 kDa polypeptide monoclonal antibodies I raised. It would also be helpful to purify similar proteins from *B. paxillifer*, and to compare characteristics of the motor proteins from different diatoms. Third, an *in vitro* assay system should be constructed to analyze detailed biochemical and biophysical characteristics of gliding motion. Inhibition of

gliding motion *in vitro* with permeabilized or opened cells by using the anti-130 kDa polypeptide antibodies might provide a critical demonstration of the involvement of the 130 kDa polypeptide in gliding motion as a power generator. As shown in this work, comparative studies between unicellular and colonial diatoms are helpful to understand molecular mechanism of gliding motion. Nowadays, new techniques for gene transfer in diatoms are becoming available. By applying these techniques, we will step into the next stage to study this unique gliding motion of the diatoms.

References

Cleveland, D. W., Fischer, S. G., Kirschner, M. W. and Laemmli, U. K. (1977). Peptide mapping by limited proteolysis in sodium dodecyl sulfate and analysis by gel electrophoresis. *J. Biol. Chem.* **252**, 1102–1106.

Cooksey, B. and Cooksey, K. E. (1980). Calcium is necessary for motility in the diatom *Amphora coffeaeformis*. *Plant Physiol.* **65**, 129-131.

De Martino, A., Meichenin A., Shi J., Pan, K. H. and Bowler, C. (2007). Genetic and phenotypic characterization of *Phaeodactylum tricornutum* (Bacillariophyceae) ccessions. *J. Phycol*. **43**, 992-1009.

Drum, R. W. and Hopkins, J. T. (1966). Diatom locomotion: An explanation. *Protoplasma* **62**, 1-33.

Edgar, L. A. (1979). Diatom locomotion: computer assisted analysis of cine film. *Br. phycol. J.* **14**, 83-101.

Edgar, L. A. and Pickett-Heaps, J. D. (1982). Ultrastructural localization of polysaccharides in the motile diatom *Navicula cuspidata*. *Protoplasma* **113**, 10-22.

Edgar, L. A. (1983). Mucilage secretions of moving diatom. *Protoplasma* **118**, 44-48.

Edgar, L. A. and Pickett-Heaps, J. D. (1983). The mechanism of diatom locomotion. I.

An ultrastructural study of the motility apparatus. *Proc. R. Soc. Lond. B* **218**, 331-343.

Edgar, L. A. and Zavortink, M. (1983). The mechanism of diatom locomotion. II. Identification of actin. *Proc. R. Soc. Lond. B* **218**, 345-348.

Edgar, L. A. and Pickett-Heaps, J. D. (1984). Diatom locomotion. *Progress in Phycological Research* **3**, 47-88.

Foth, B. J., Goedecke, M. C. and Soldati, D. (2006). New insights into myosin evolution and classification. *Proc. Natl. Acad. Sci. USA* **103**, 3681–3686.

Gupta, G. and Agrawal, S. C. (2007). Survival and motility of diatoms *Navicula grimmei* and *Nitzschia palea* affected by some physical and chemical factors. *Folia Microbiol*. **52**, 127-134.

Harper, M. A. and Harper J. F. (1967). Measurements of diatom adhesion and their relationship with movement. *Br. Phycol. Bull.* **3**, 195-207.

Heintzelman, M. B. and Enriquez, M. E. (2010). Myosin diversity in the diatom *Phaeodactylum tricornutum*. *Cytoskeleton* **67**, 142-151.

Inoue, T. and Osatake, H. (1988). A new drying method of biological specimens for scanning electron microscopy; the *t*-butyl alcohol freeze-drying method. *Arch. Histol. Cytol.* **51**, 53-59.

Jahn, R. and Schmid, A. M. (2007). Revision of the brackish-freshwater diatom genus *Bacillaria* Gmelin (Bacillariophyta) with the description of a new variety and two new species. *Eur. J. Phycol.* **42**, 295-312.

Kapinga, M. R. M. and Gordon, R. (1992). Cell motility rhythms in *Bacillaria paxillifer*. *Diatom Research* **7**, 221-225.

Kimura, K. and Tomaru, Y. (2015). Discovery of two novel viruses expands the diversity of single-stranded DNA and single-stranded RNA viruses infecting a cosmopolitan marine diatom. *Appl. Environ. Microbiol.* **81**(3), 1120-1131.

Köhler G. and Milstein C. (1975). Continuous cultures of fused cells secreting antibody of predefined specificity, *Nature* **256**, 495-497.

Lewin, J. C., Lewin R. A. and Philpott D. E. (1958). Observations of *Phaeodactylum tricornutum*. *J. Gen. Microbiol.* **18**, 418-426.

Lewin, J. C. (1958). The taxonomic position of *Phaeodactylum tricornutum*. *J. Gen. Microbiol.* **18**, 427-432.

Lind, J. L., Heimann, K., Miller, E. A., Vliet, C. V., Hoogenraad, N. J. and Wetherbee, R. (1997). Substratum adhesion and gliding in a diatom are mediated by extracellular proteoglycans. *Planta* **203**, 213-221.

McConville, M. J., Wetherbee., R. and Bacic, A. (1999). Subcellular location and composition of the wall and secreted extracellular sulphated polysaccharides /proteoglycans of the diatom. *Protoplasma*, **206**, 188-200.

Montsant, A., Allen, A. E., Coesel, S., De Martino, A., Falciatore, A., Mangogna, M., Siaut, M., Heijde, M., Jabbari, K., Maheswari, U., Rayko, E., Vardi, A., Apt, K. E., Berges, J. A., Chiovitti, A., Davis, A. K., Thamatrakoln, K., Hadi, M. Z., Lane, T. W., Lippmeier, J. C., Martinez, D., Parker, M. S., Pazour, G. J., Saito, M. A., Rokhsar, D. S., Armbrust, E. V. and Bowler, C. (2007). Identification and comparative genomic analysis of signaling and regulatory components in the diatom *Thalassiosira pseudonana*. *J. Phycol.* **43**, 585–604.

Mùller, O. F. (1782). Von einem sonderbaren Wesen im Meerwasser, welches aus kleinen Stäbgen, durch deren mancherley Stellung es verschiedene Gestalten bildet, zu bestehen scheint. Goee, J. A. E. edts., *Otto Friedrich Mùllers kleine Schriften aus der Naturhistorie*, Dessau, Germany; I. Band, Kap.**1**: 1-14.

Mùller, O. F. (1783). Om et besonderligt Vaesen i Strandvandet. (Laest 7.12.1781). *Danske Videnskabernes Selskabs Skirifter aus der Naturhistorie*.Gopenhagen **2**:277-286.

Pickett-Heaps, J., Hill, D. R. A. and Blaze, K. L. (1991). Active gliding motility in an araphid marine diatom, *Ardissonea* (formerly *Synedra*) *crystallina*. *J. Phycol.* **27**, 718-725.

Poulsen, N. C., Spector, I., Spurck, T. P., Schultz, T. F. and Wetherbee, R. (1999). Diatom gliding is the result of an actin-myosin motility system. *Cell Motil. Cytoskel.* **44**, 23-33.

Rasband, W. S. (1997-2014). *ImageJ,* U. S. National Institutes of Health, Maryland, USA. http://imagej.nih.gov/ij/

Reynolds, E. S. (1963). The use of lead citrate at high pH as an electron-opaque stain in electron microscopy. *J. Cell Biol*. **17**, 208-212.

Round, F. E., Crawford, R. M. and Mann, D. G. (1990). *The Diatoms. Biology and Morphology of the Genera.* Cambridge University Press, Cambridge. 760 p.

Schmid, A. M. (2007). The "paradox" diatom *Bacillaria paxillifer* (Bacillariophyta) revisited. *J. Phycol.* **43**, 139-155.

Spudich, J. A. and Watt, S. (1971). The regulation of rabbit skeletal muscle contraction. *J. Biol. Chem.* **246**, 4866-4871.

Umemoto, S. and Sellers, J. R. (1990). Characterization of *in vitro* motility assays using smooth muscle and cytoplasmic myosins. *J. Biol. Chem.* **265**, 14864-14869.

Warshaw, D. M., Desrosiers, J. M., Work, S. S. and Trybus, K. M. (1990). Smooth muscle myosin cross-bridge interactions modulate actin filament sliding velocity *in vitro*. *J. Cell Biol.* **111**, 453-463.

Webster, D. R., Cooksey, K. E. and Rubin, R. W. (1985). An investigation of the involvement of cytoskeletal structures and secretion in gliding motility of the marine diatom, *Amphora coffeaeformis*. *Cell motility*, **5**, 103-122.

Wells, A. L., Lin, A. W., Chen, L. Q., Safer, D., Cain, S. M., Hasson, T., Carragher, B. O., Milligan, R. A. and Sweeney, H. L. (1999). Myosin VI is an actin-based motor that moves backwards. *Nature* **401**, 505-508.

Wetherbee, R., Lind, J. L., Burke, J. and Quatrano, R. S. (1998). The first kiss: establishment and control of initial adhesion by raphid diatoms. *J. Phycol.* **34**, 9-15.